Projects SKYSURF and WebbSURF: Diffuse Light Constraints from HST and JWST at 1 AU

Rogier Windhorst (ASU) — JWST Interdisciplinary Scientist

+ HST SKYSURF & JWST PEARLS teams: T. Carleton, R. O'Brien, S. Cohen, R. Jansen, D. Kramer, I. McIntyre, J. Summers, S. Tompkins, C. Conselice, J. Diego, S. Driver, H. Yan, D. Coe, B. Frye, N. Grogin, A. Koekemoer, M. Marshall, N. Pirzkal, A. Robotham, R. Ryan Jr., C. Willmer+

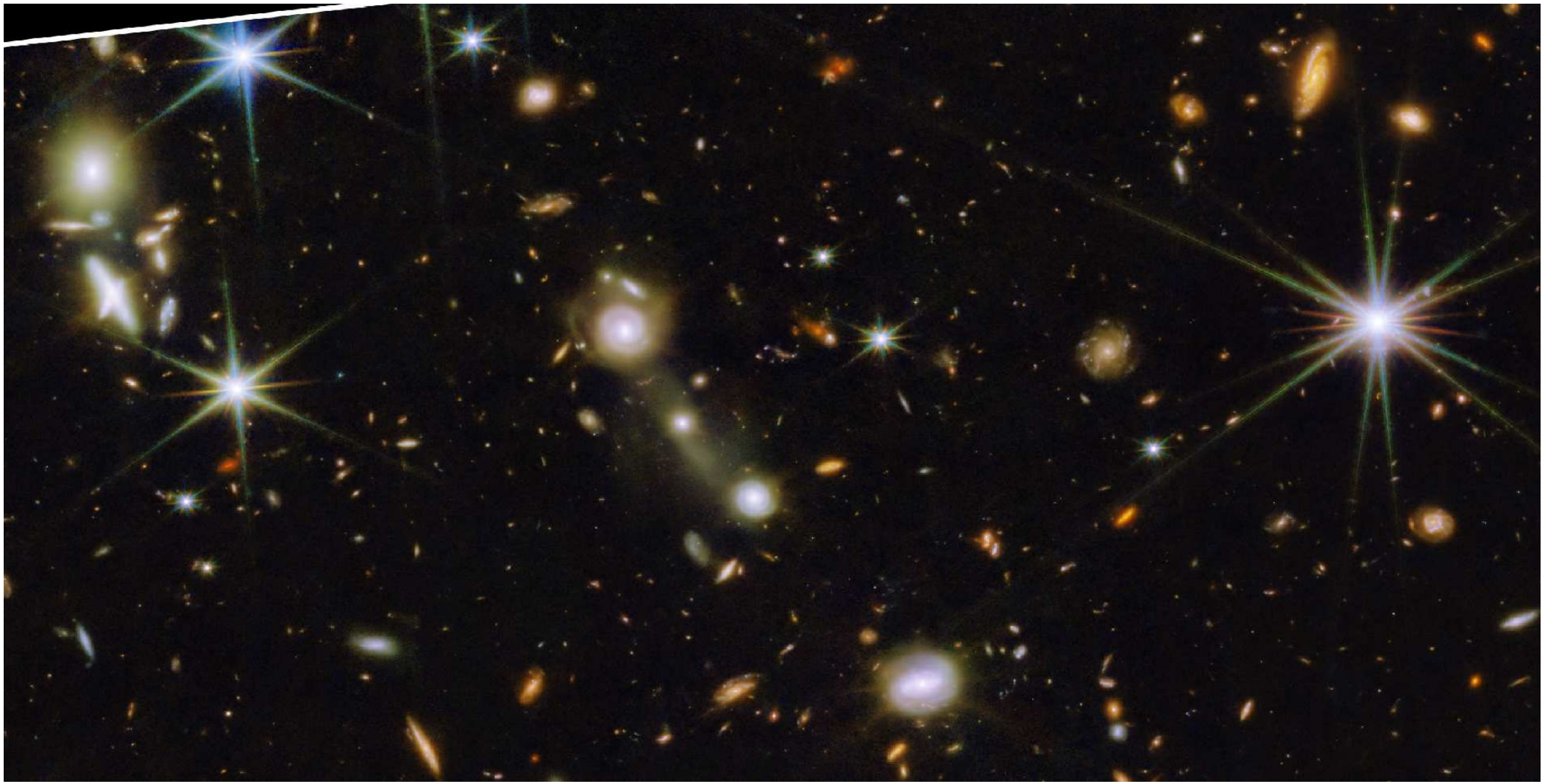

Talk at the University of Manchester, UK, Mo Apr. 24, 2023

PDF on: http://www.asu.edu/clas/hst/www/jwst/skysurf_webbsurf_manchester23.pdf

Outline and Conclusions

- (1) Summary of the HST SKYSURF project and Diffuse Light
- (2) Summary of the JWST PEARLS project and Diffuse Light
- (3) Combined Limits to Diffuse Light at 0.9–4.5 μm

Some remarkable results in PEARLS and other JWST projects:

- Abundance of red (dusty) spirals, $\sim$30% more spirals than seen by HST
- Accurate 0.9-5 μm galaxy counts to AB$\lesssim$28.5–29 mag.
- (Old SED) tidal tails everywhere: $\lesssim$20% of Integrated Galaxy Light (IGL).
- Webb 0.9–5 μm Diffuse Light limits to $\lesssim$10% of Zodiacal.
- HST 1.25–1.6 μm Diffuse Light limits to $\lesssim$7% of Zodiacal.

SKYSURF-1: Windhorst, Carleton, O'Brien et al. (2022, AJ, 164, 141; astro-ph/2205.06214)

SKYSURF-2: Carleton, Windhorst, O'Brien et al. (2022, AJ, 164, 170; astro-ph/2205.06347)

SKYSURF-3: Kramer, Carleton, Cohen, et al. (2022, ApJL, 940, L15; astro-ph/2208.07218v2)

SKYSURF-4: O'Brien, Carleton, Windhorst, et al. (2023, AJ, in press; astro-ph/2210.08010)

PEARLS/WebbSURF: Windhorst, Cohen, Jansen et al. (2023, AJ, 165, 13; astro-ph/2209.04119)

Galactic plane and the Zodiacal disk at night:

They are inclined by 60°.

SKYSURF aims to map both their diffuse light across the sky.

JWST is now doing the same, but in much darker 0.9-5 μm L2 skies.

More than 95% of photons in STScI Archive (outside the Galactic plane; $|b^{II}| \gtrsim 25°$) come from distances D$\lesssim$5 AU.

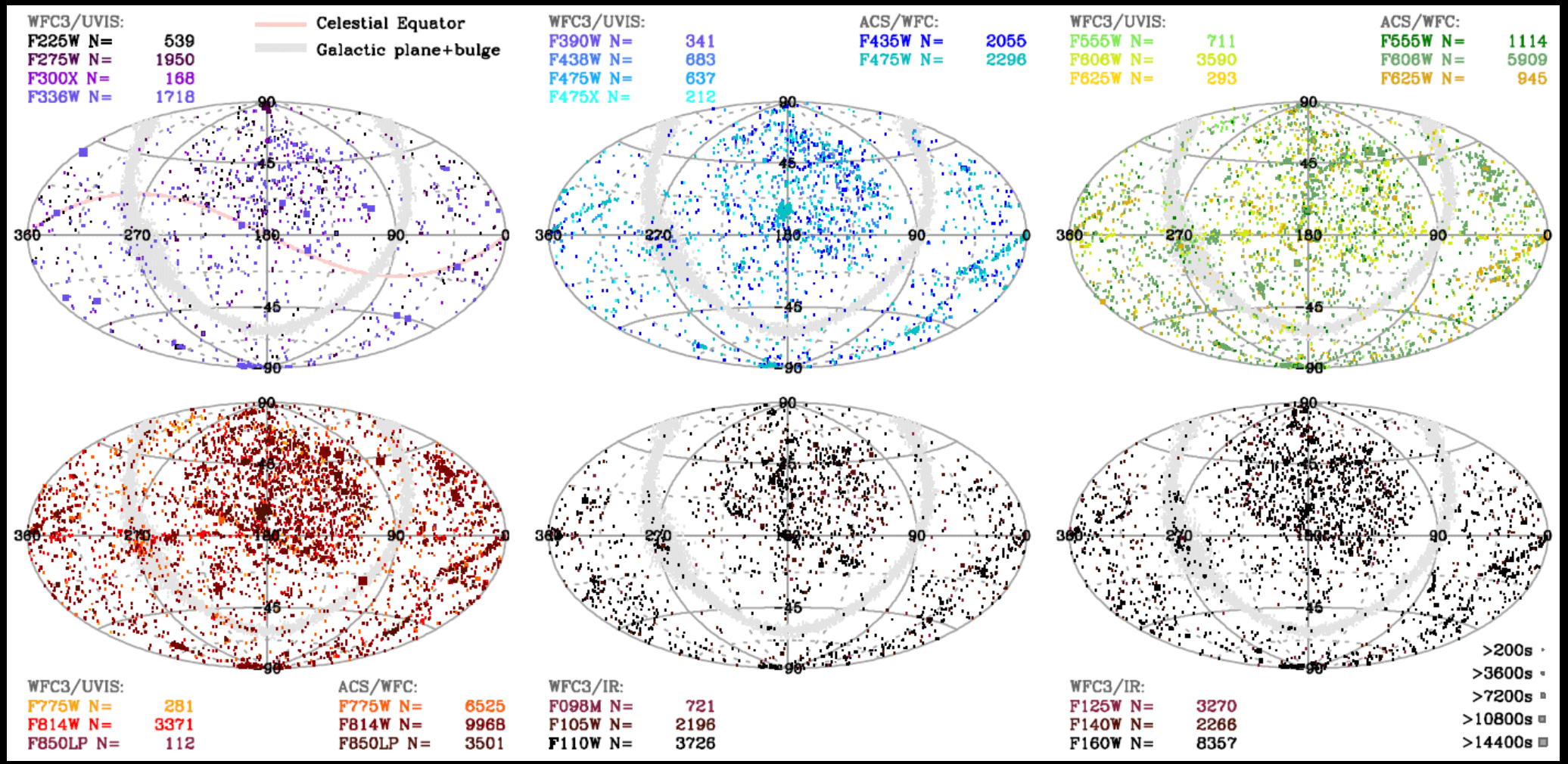

SKYSURF's database: 249,861 exposures (878,000 readouts) in 16,822 HST field-of-views (FOVs) taken over 28 years.

28 filters from 0.2-1.6 μm; with 12 main broad-band filters in $\sim$1400 independent HST fields.

Tim Carleton, Rosalia O'Brien: database lead. UGs built database in 2020.

- How SKYSURF measures sky brightness (SB) & identifies straylight

In all SKYSURF images we need to identify straylight from:

1) Earthshine [Limb Angle]; 2) Sunlight [Sun Angle and Sun Altitude above Earth]; 3) Moonlight [Moon Angle] (Sarah Caddy).

(Earth's Limb is down 24° from LEO orbital vector due to Earth curvature).

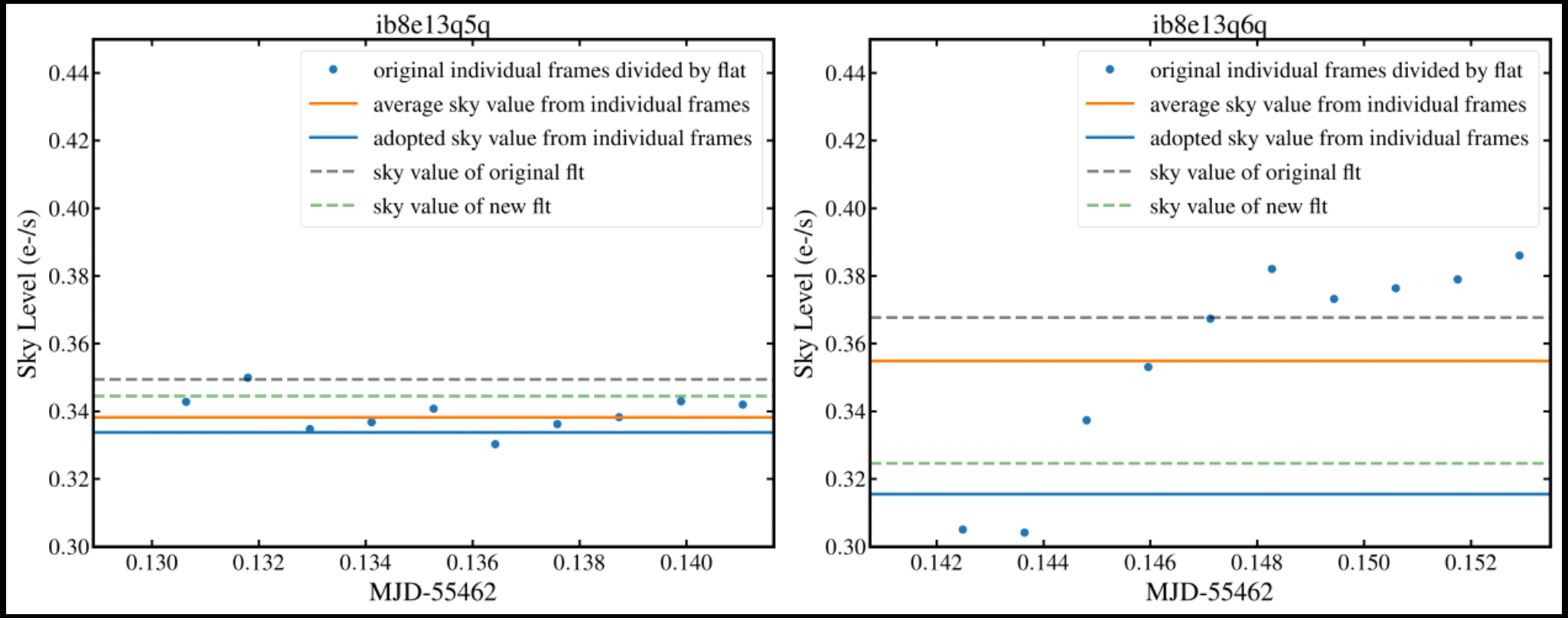

- SKYSURF's 50,073 WFC3/IR exposures are split into $\gtrsim$400,000 on-the-ramp sub-exposures (Carleton et al.) — we are not lacking statistics.

- These (+all 210,000 sub-orbital CCD exposures) allow us to monitor sky-SB vs. HST's orbital phase [Left: Start; Right: End of orbit].

- Critical for flagging & removing SKYSURF exposures with straylight.

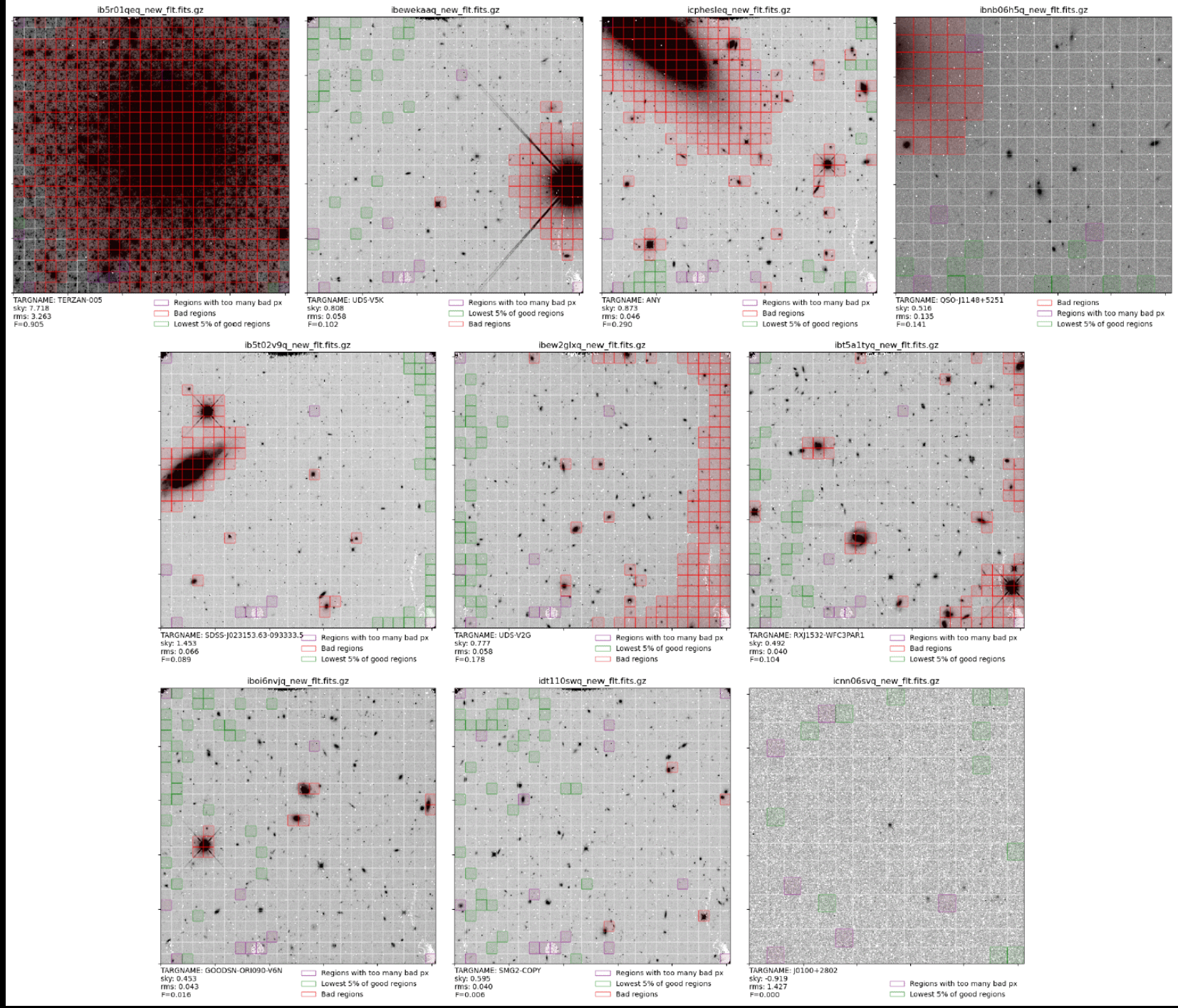

First, identify all sub-grid regions with objects or defects (R. O'Brien).

5% of object-free boxes give best match with simulated sky-SB (D. Carter).

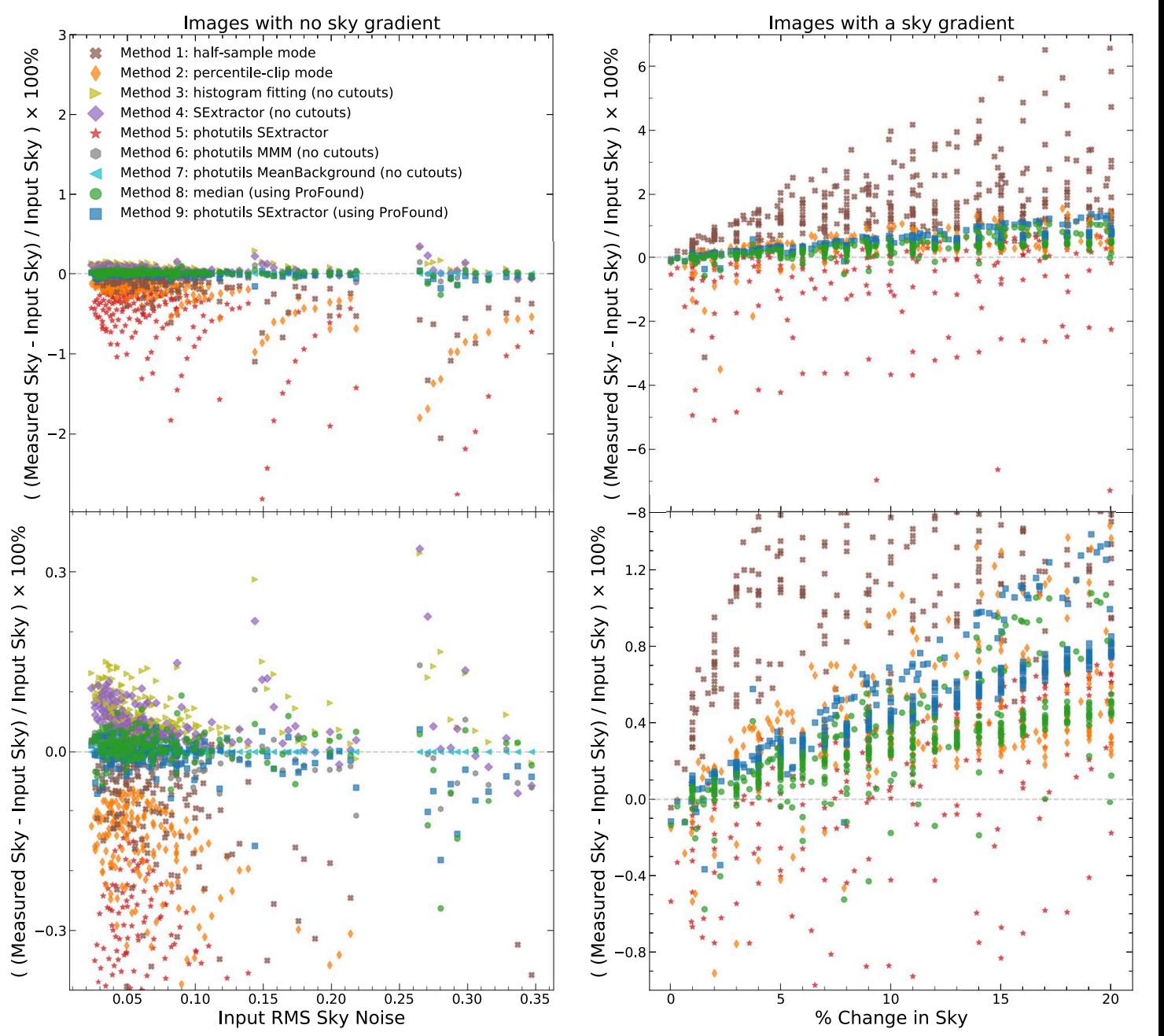

Top: Relative error in Measured / Simulated sky-SB in %;

Bottom: same but enlarged;

Left: simulated without gradients;

Right: images with 5–20% (straylight) gradients.

(Real Zodiacal gradients are always less across HST FOVs).

W/O gradients: Best 3 out of 9 algorithms recover sky-SB $\lesssim$0.1-0.2%.

With 5–10% gradients: recover sky-SB $\lesssim$0.4% (Carter, O'Brien).

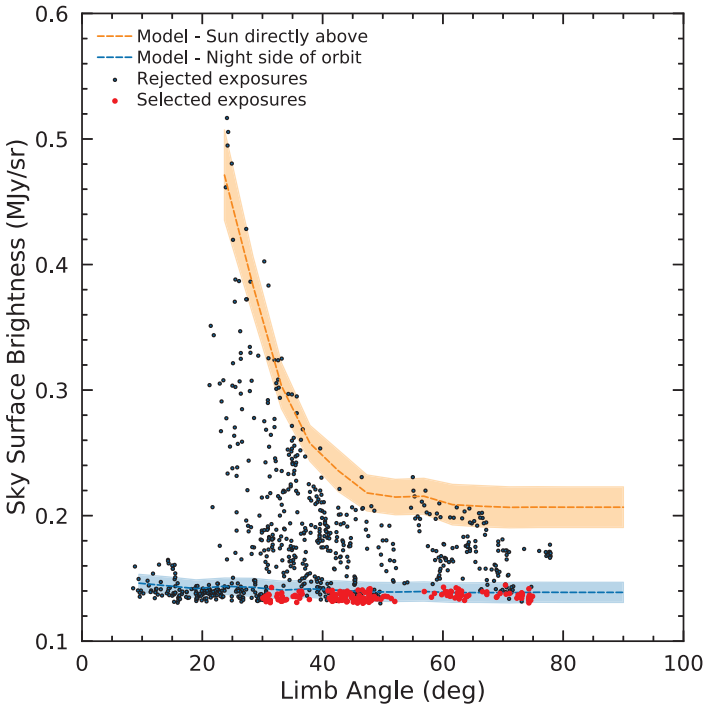

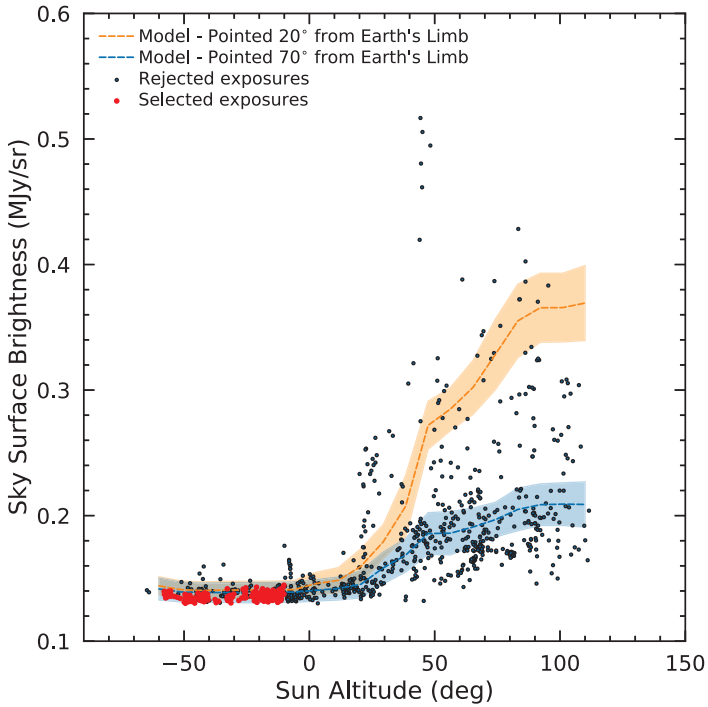

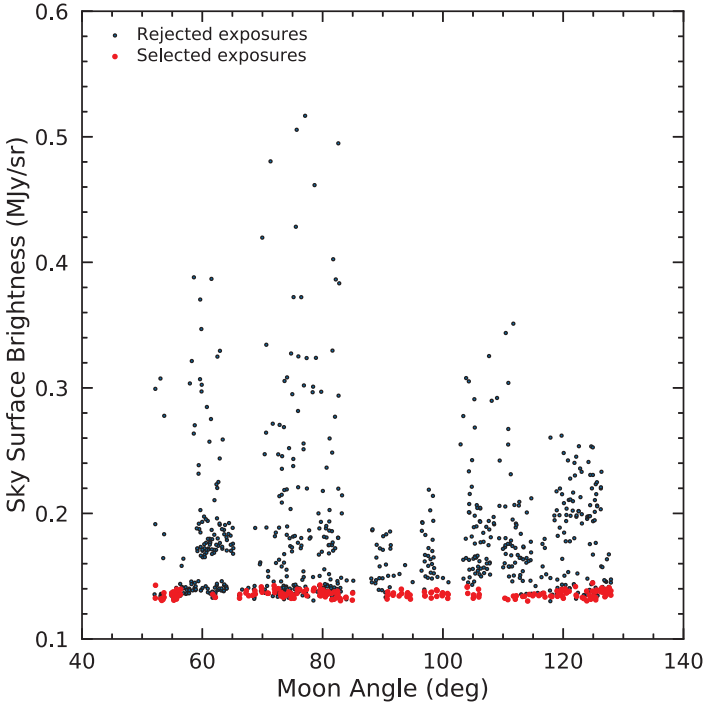

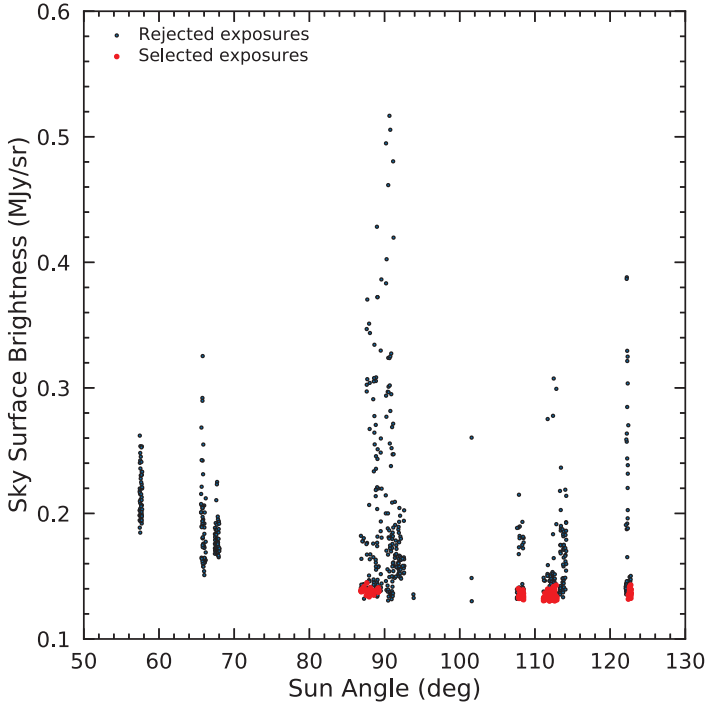

Sarah Caddy's study to minimize straylight:

(a) Earth Limb Angle LA$\gtrsim$30–40° to avoid Earthshine; *and*

(b) Sun Altitude above Earth $\alpha_\odot \lesssim$–10° (orbital night side) minimizes Sunlight scattered off the bright Earth; *and*

(c) The Moon Angle MA$\gtrsim$50 °; *and*

(d) Sun Ang. SA$\gtrsim$80° avoids straylight into the HST optics.

SKYSURF's high-fidelity sample applies all these constraints (R. O'Brien).

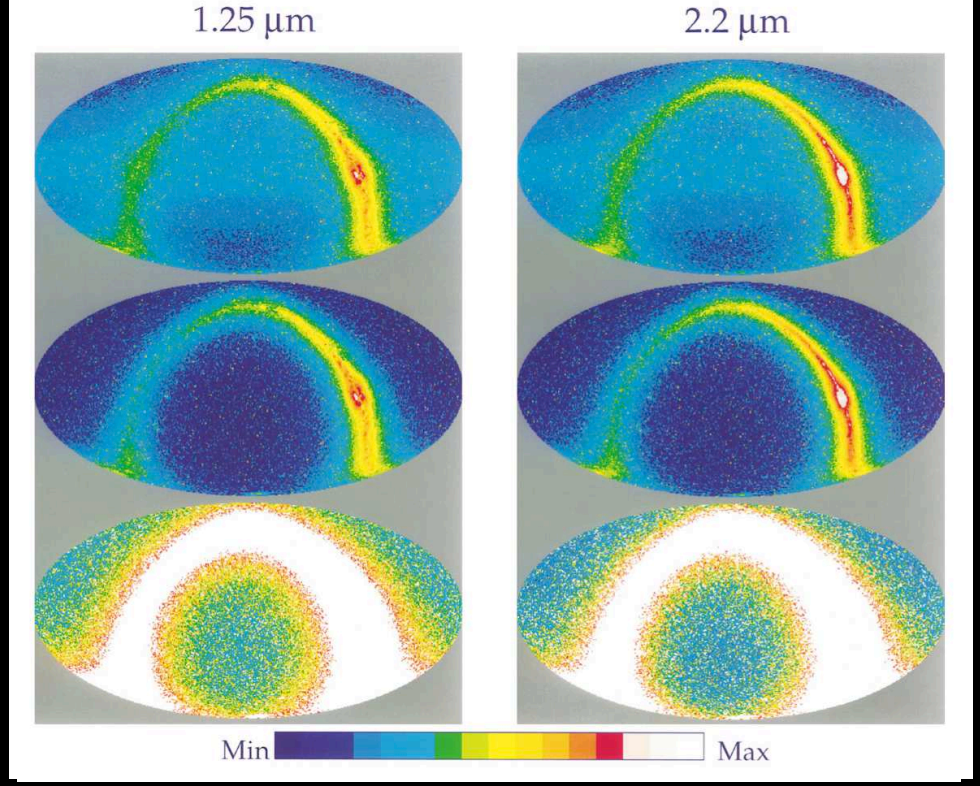

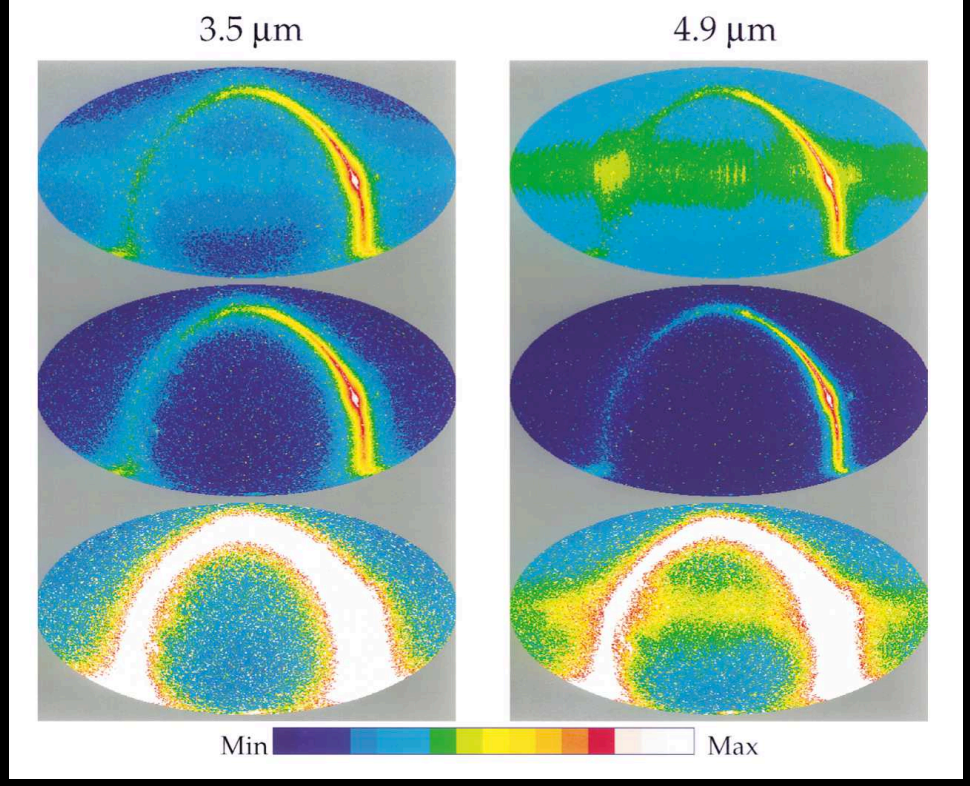

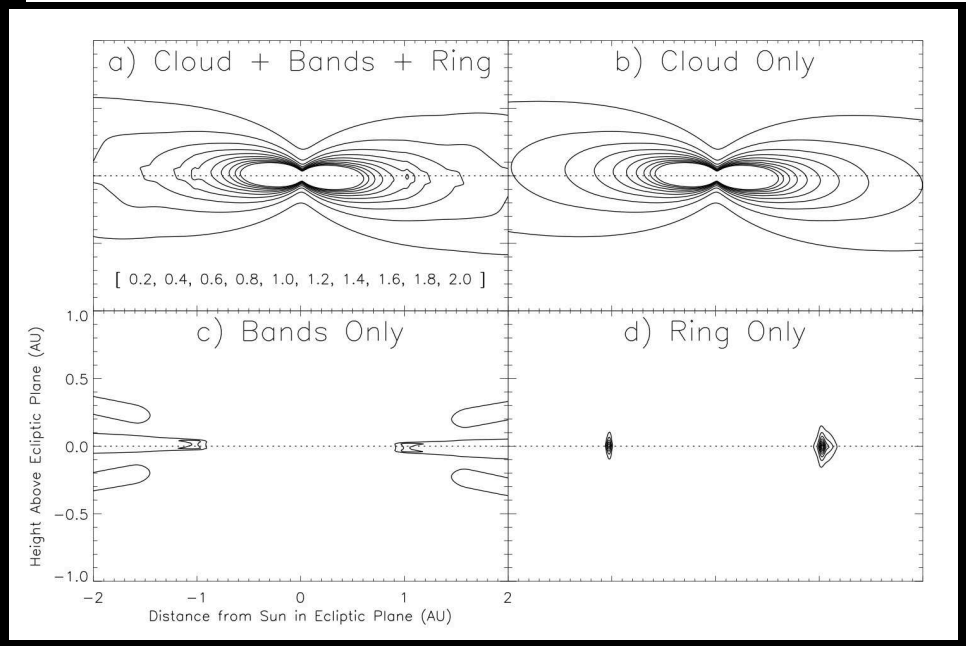

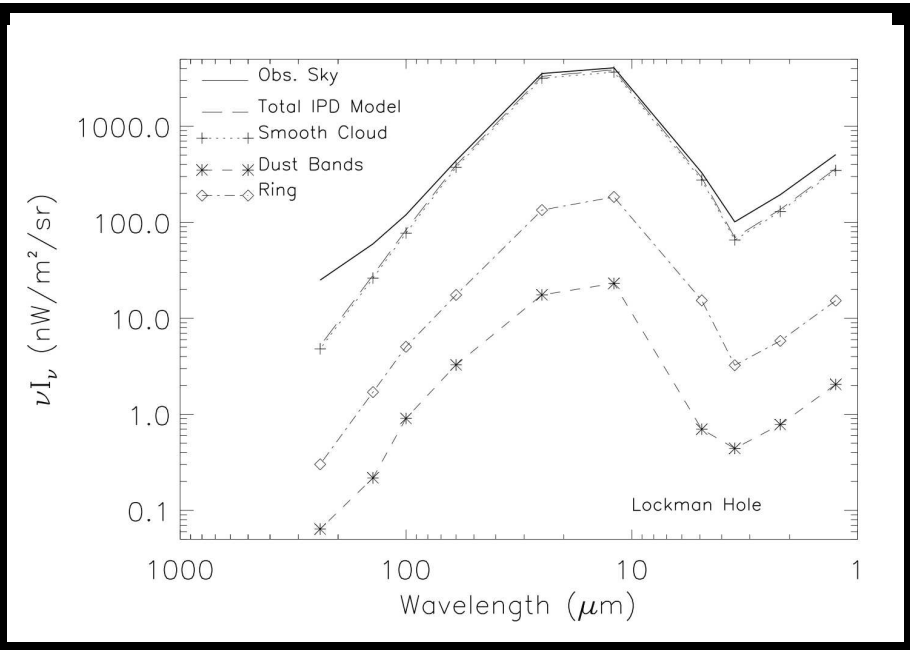

Kelsall (1998) Zodi model based on Cosmic Background Explorer data.

We'll show that compared to HST, Kelsall misses significant 1-2 μm sky-SB.

- How SKYSURF measures residual sky compared to Zodiacal models

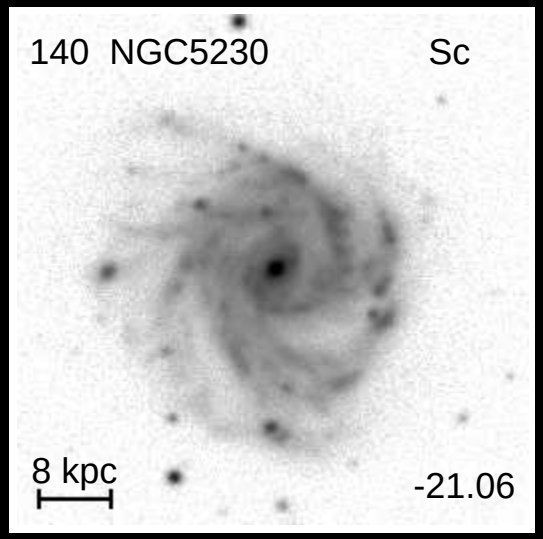

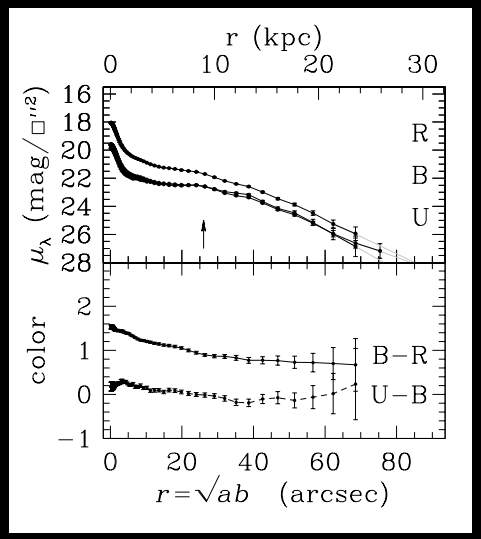

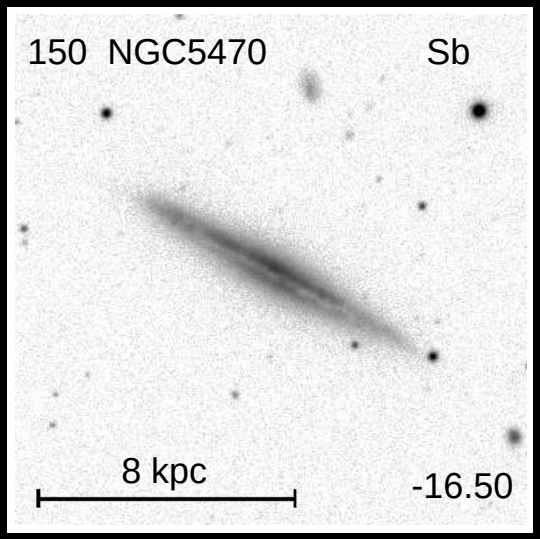

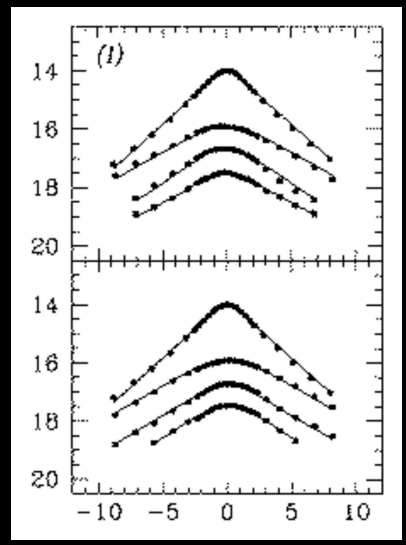

[Left]: Face-on disks: *exponential radial* light-profiles (Jansen^{+} 2000).

[Right]: Edge-on disks: *vertical sech* light-profiles (de Grijs^{+} 1997).

For Zodiacal disk-SB we use: sech(z) = [exp(z) + exp(-z)] / 2, which provide remarkable good fits to both dimmest HST data and Zodi models!

The (observed–model) sky-SB lets SKYSURF identify diffuse light sources:

1) Residual instrumental effects; 2) Diffuse ZL component not in the model;

3) Diffuse Galactic Light (DGL); 4) Diffuse EBL between discrete galaxies.

(1) SKYSURF's first results and estimates of diffuse 1.25-1.6 μm light

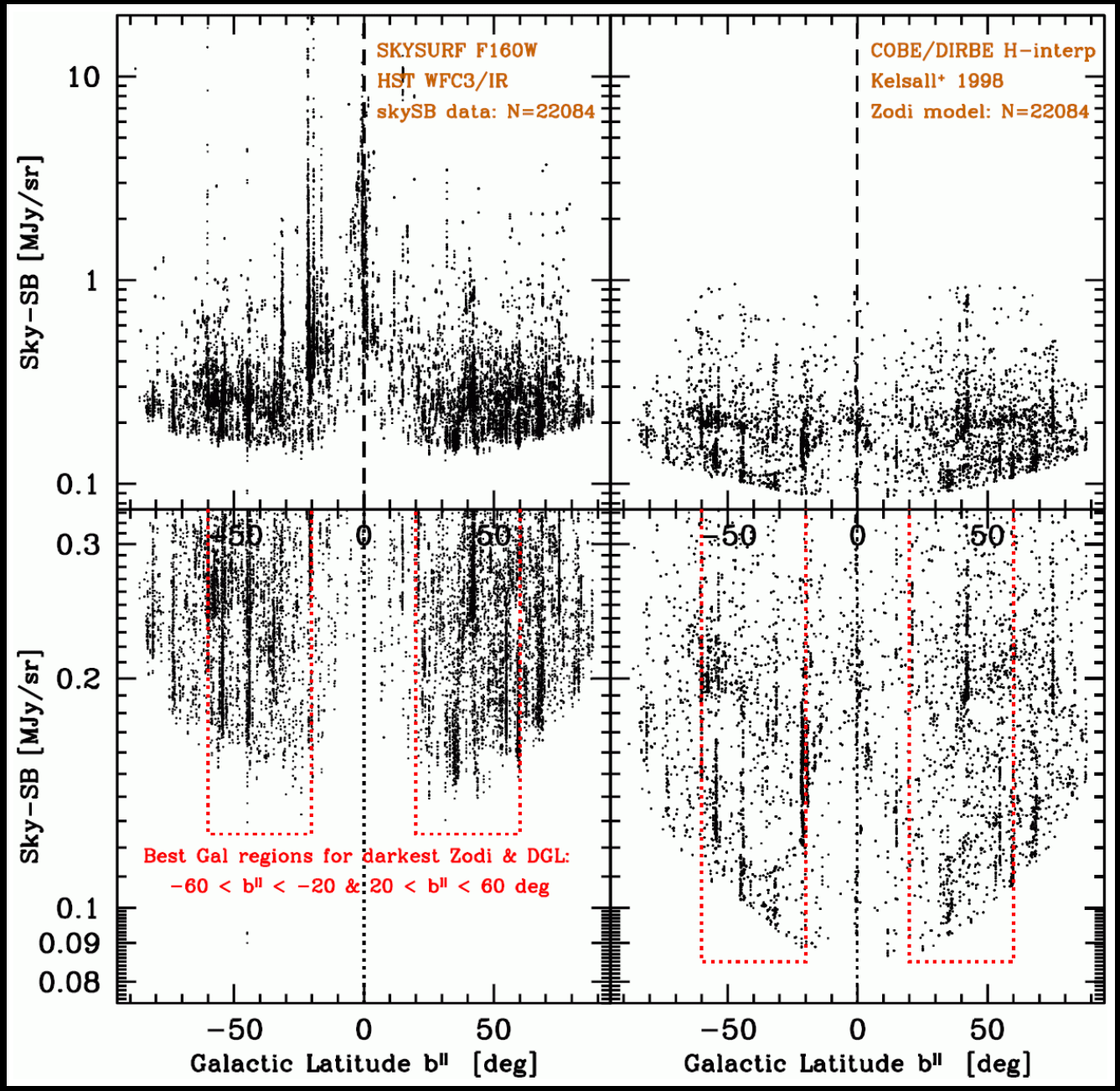

[Left]: 1.60 μm HST sky-SB; [Right]: Kelsall model for $same$ (RA, Dec, t).

First, identify $darkest$ regions in Galactic coordinates ($20° \lesssim |b^{II}| \lesssim 60°$).

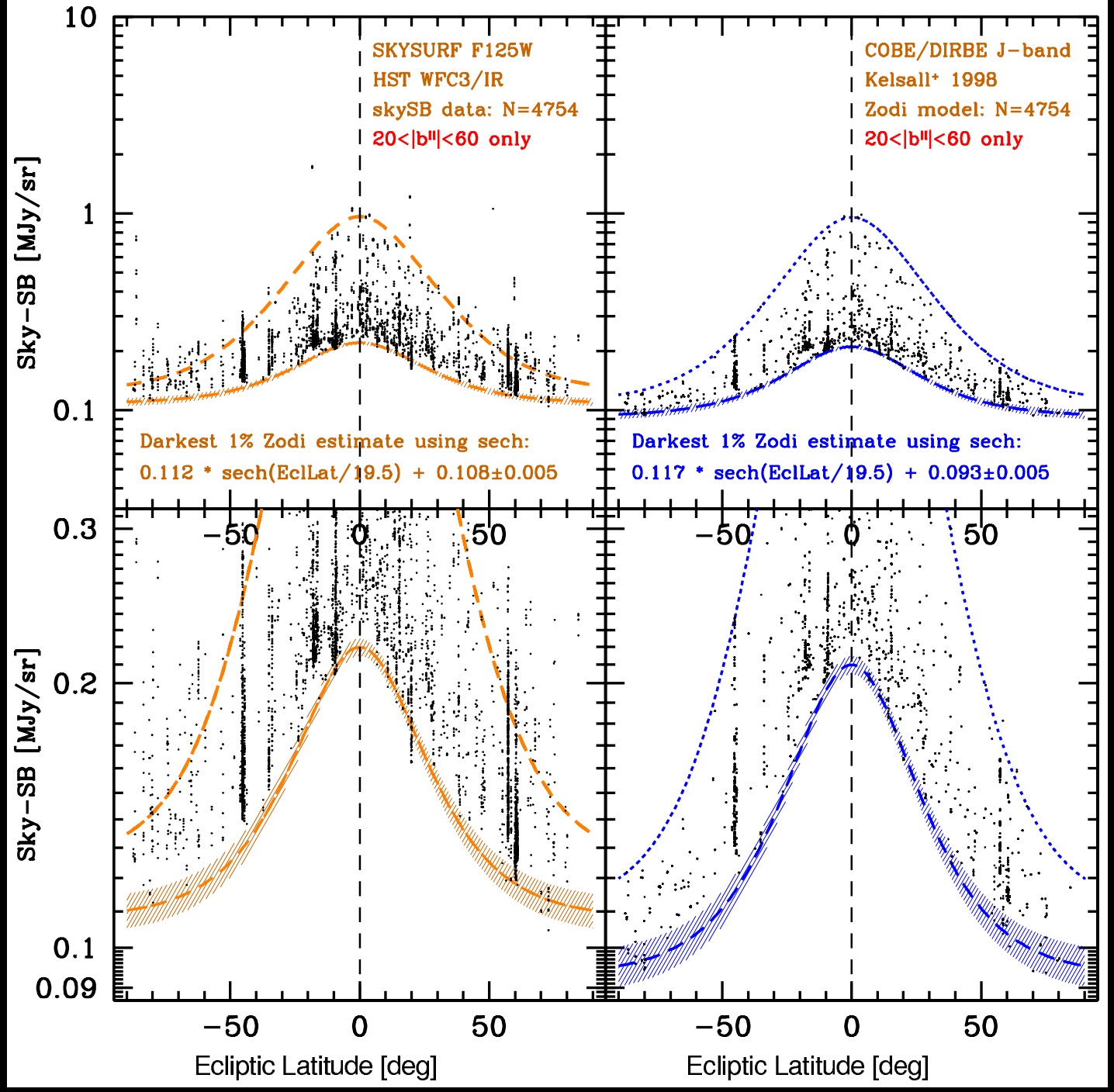

1.25 μm HST+Kelsall vs. b^{Ecl}: $sech$+error = lowest 1% of sky-SB.

Lowest 1% Δ(HST–Kelsall)$\simeq$0.015$\pm$0.008 MJy/sr at darkest Galactic.

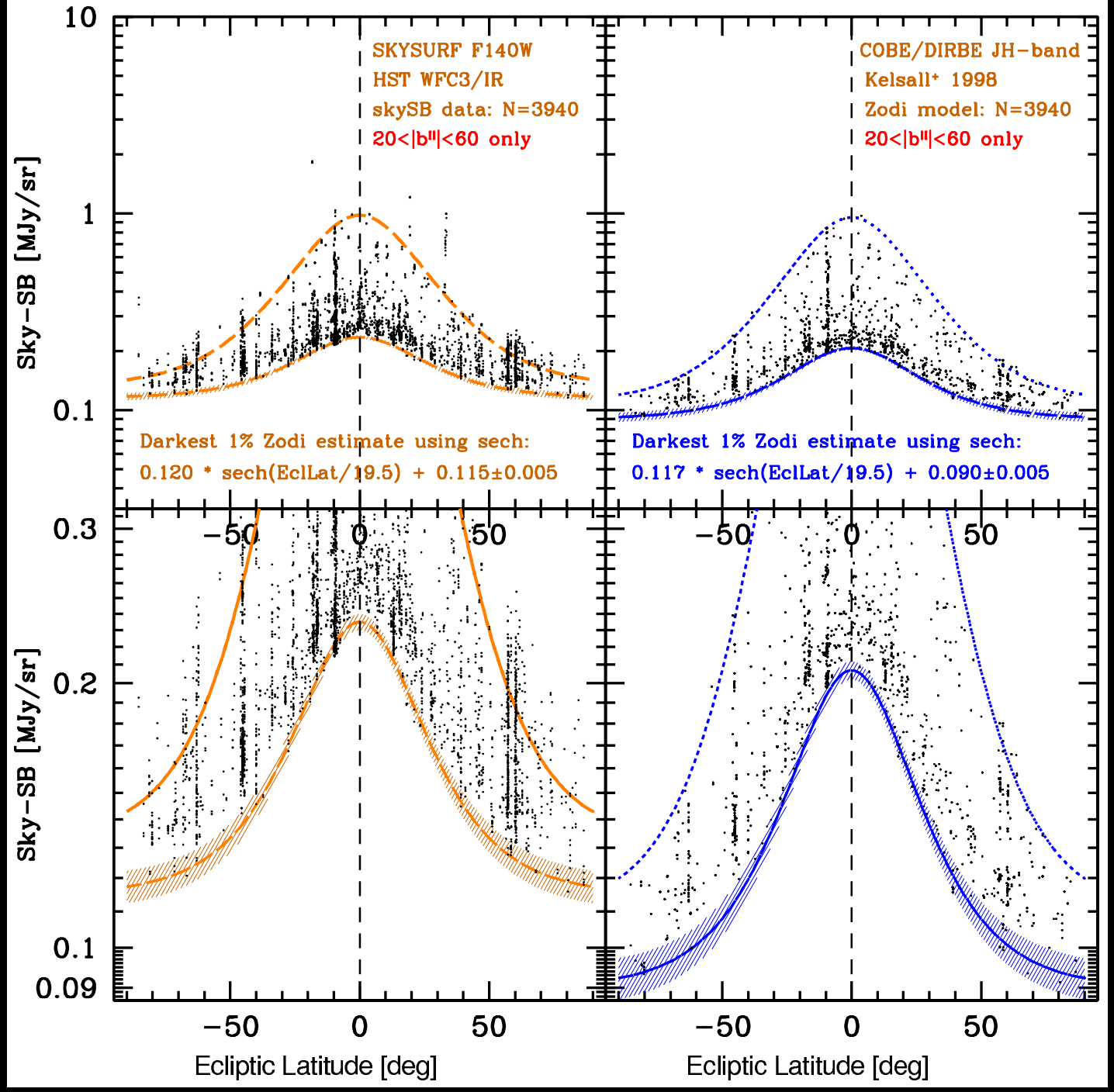

1.40 μm HST+Kelsall vs. b^{Ecl}: $sech$+error = lowest 1% of sky-SB.

Lowest 1% Δ(HST–Kelsall)$\simeq$0.025$\pm$0.009 MJy/sr at darkest Galactic.

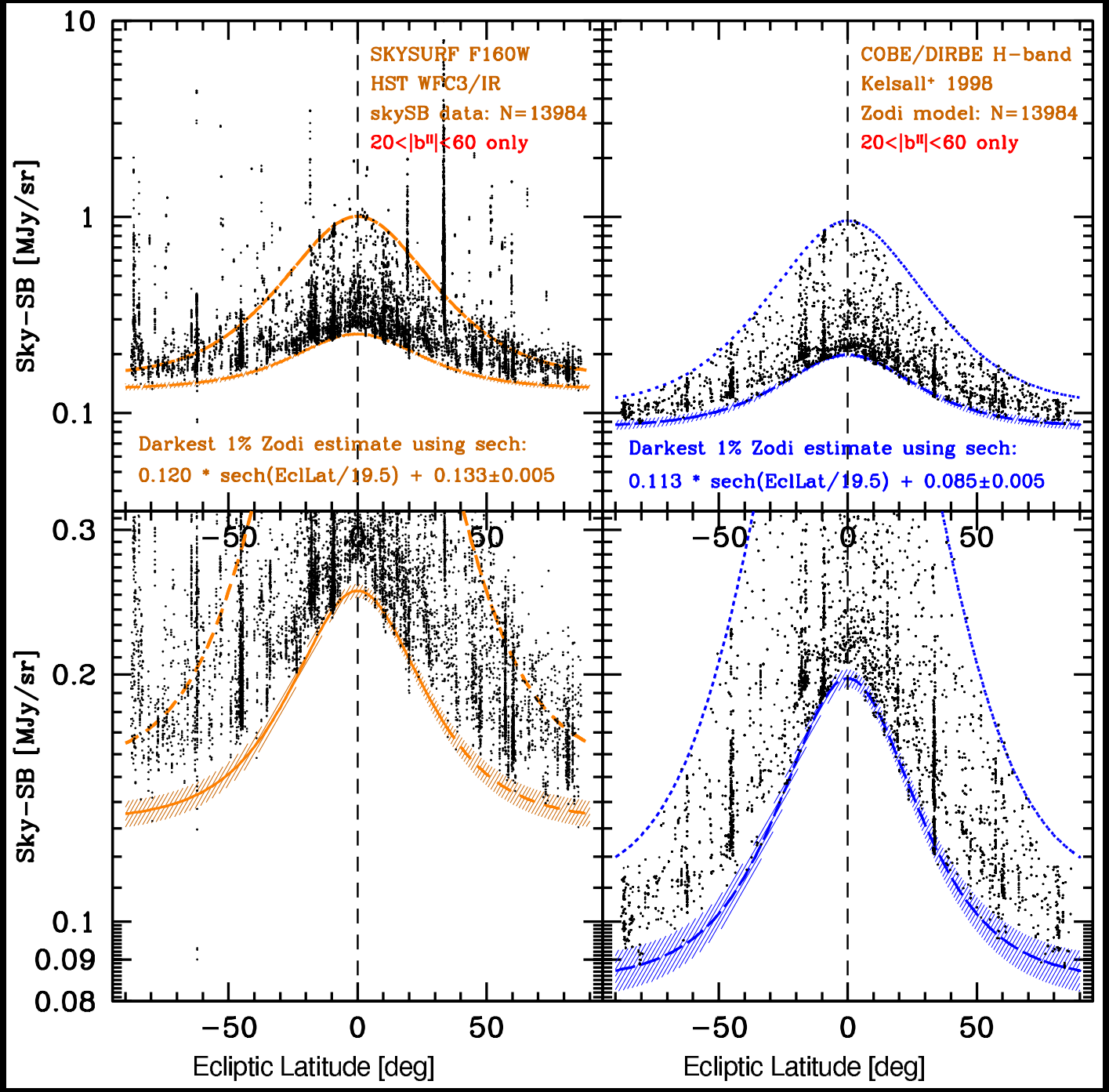

1.60 μm HST+Kelsall vs. b^{Ecl}: $sech$+error = lowest 1% of sky-SB.

Lowest 1% Δ(HST−Kelsall)$\simeq$0.048$\pm$0.009 MJy/sr at darkest Galactic.

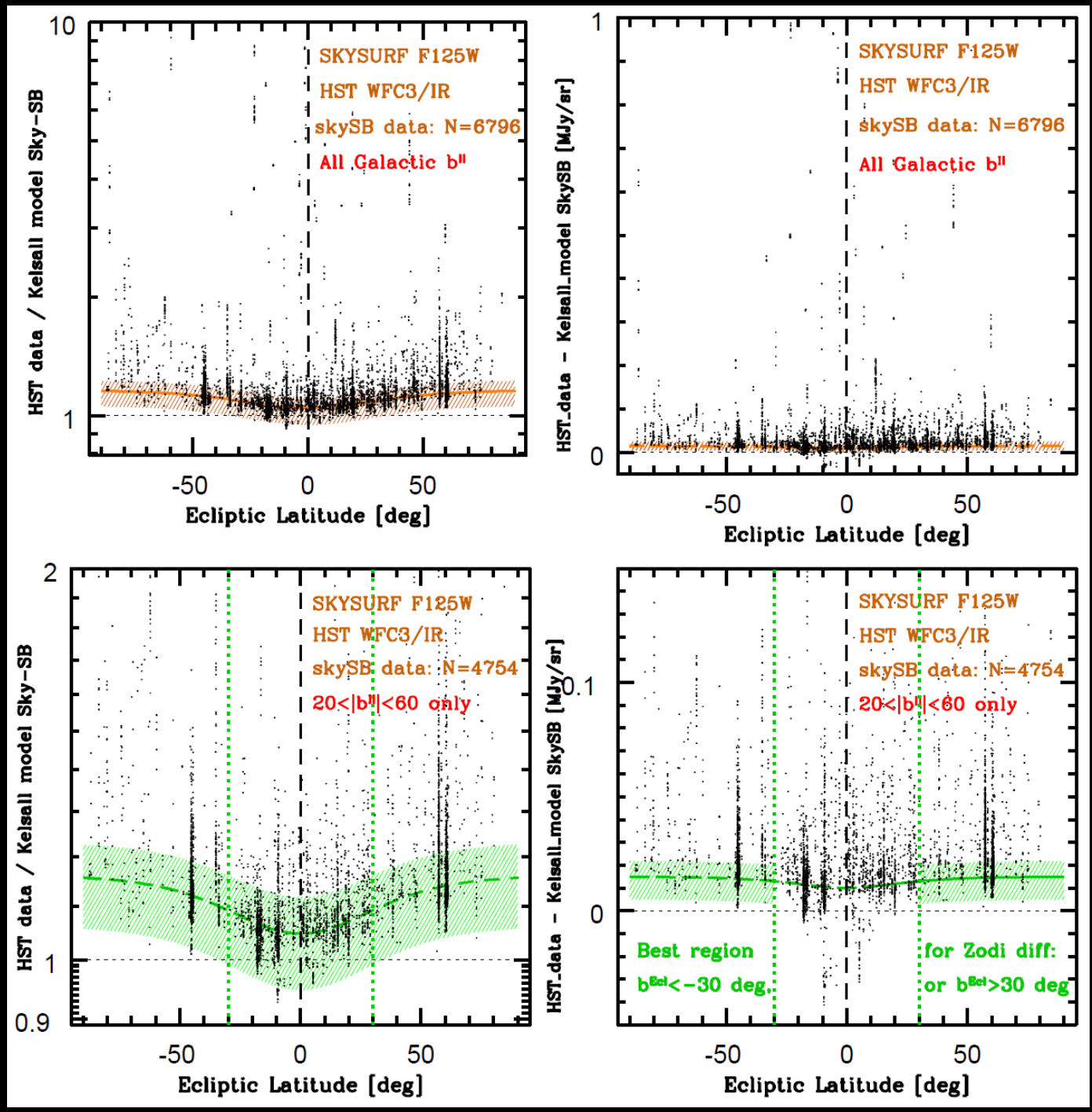

1.25 μm [Left]: HST/Kelsall ratio vs. b^{Ecl}; [Right] HST–Kelsall difference.

Linear offset Δ(HST–Kelsall)$\simeq$0.015$\pm$0.008 MJy/sr remains best fit.

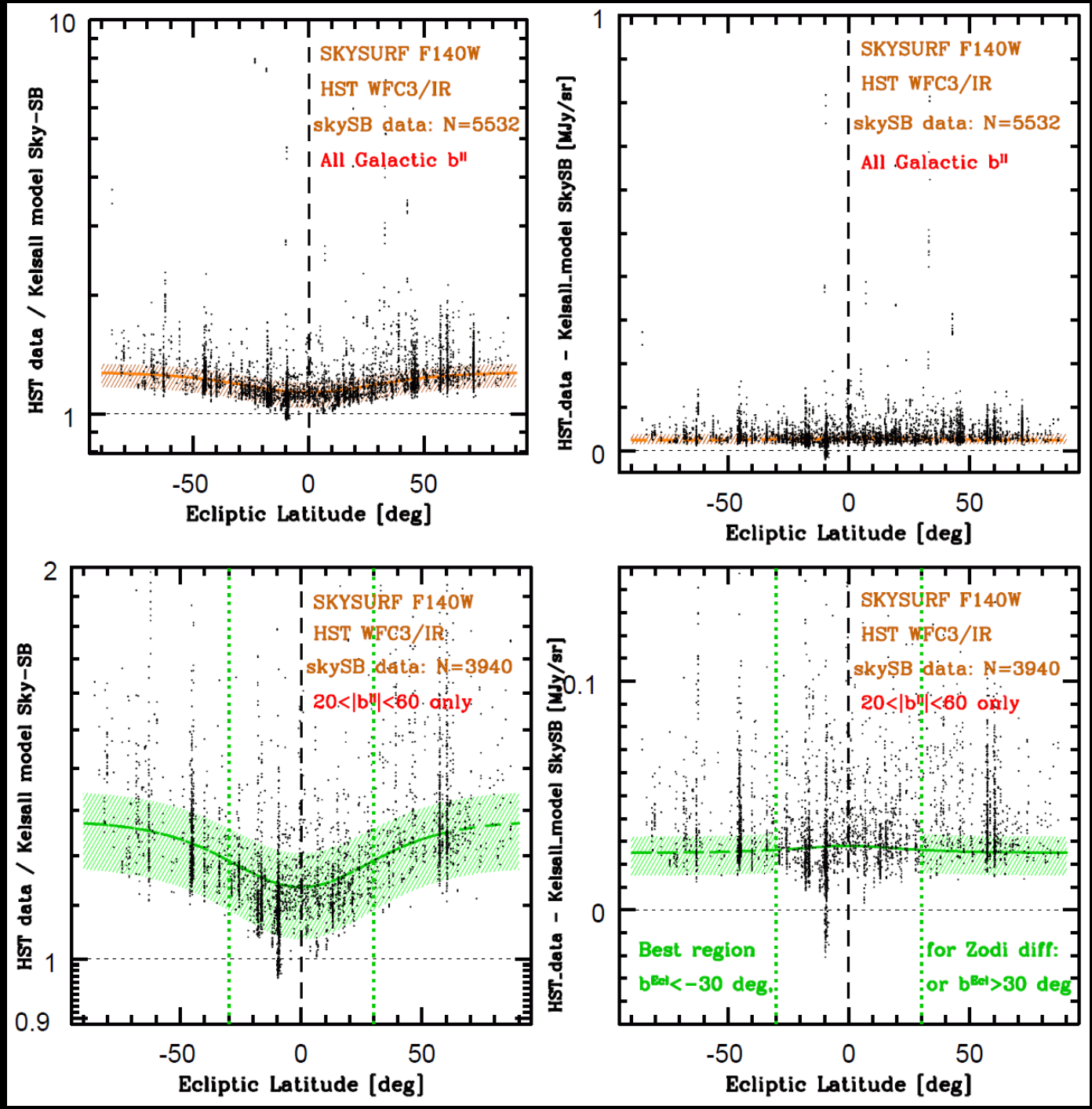

1.40 μm [Left]: HST/Kelsall ratio vs. b^{Ecl}; [Right] HST–Kelsall difference.

Linear offset Δ(HST–Kelsall)$\simeq$0.025$\pm$0.009 MJy/sr remains best fit.

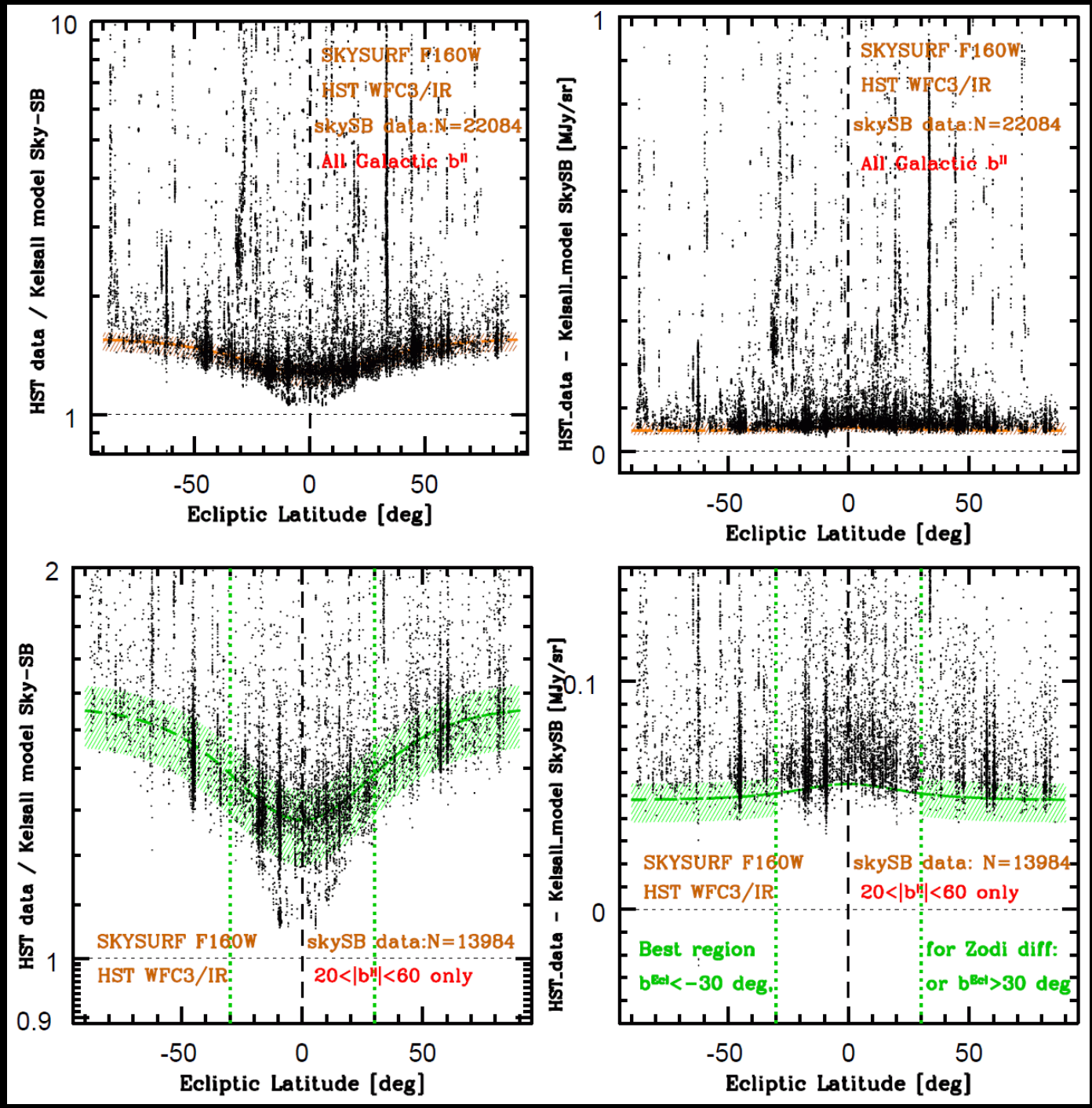

1.60 μm [Left]: HST/Kelsall ratio vs. b^{Ecl}; [Right] HST–Kelsall difference.

Linear offset Δ(HST–Kelsall)$\simeq$0.048$\pm$0.009 MJy/sr remains best fit.

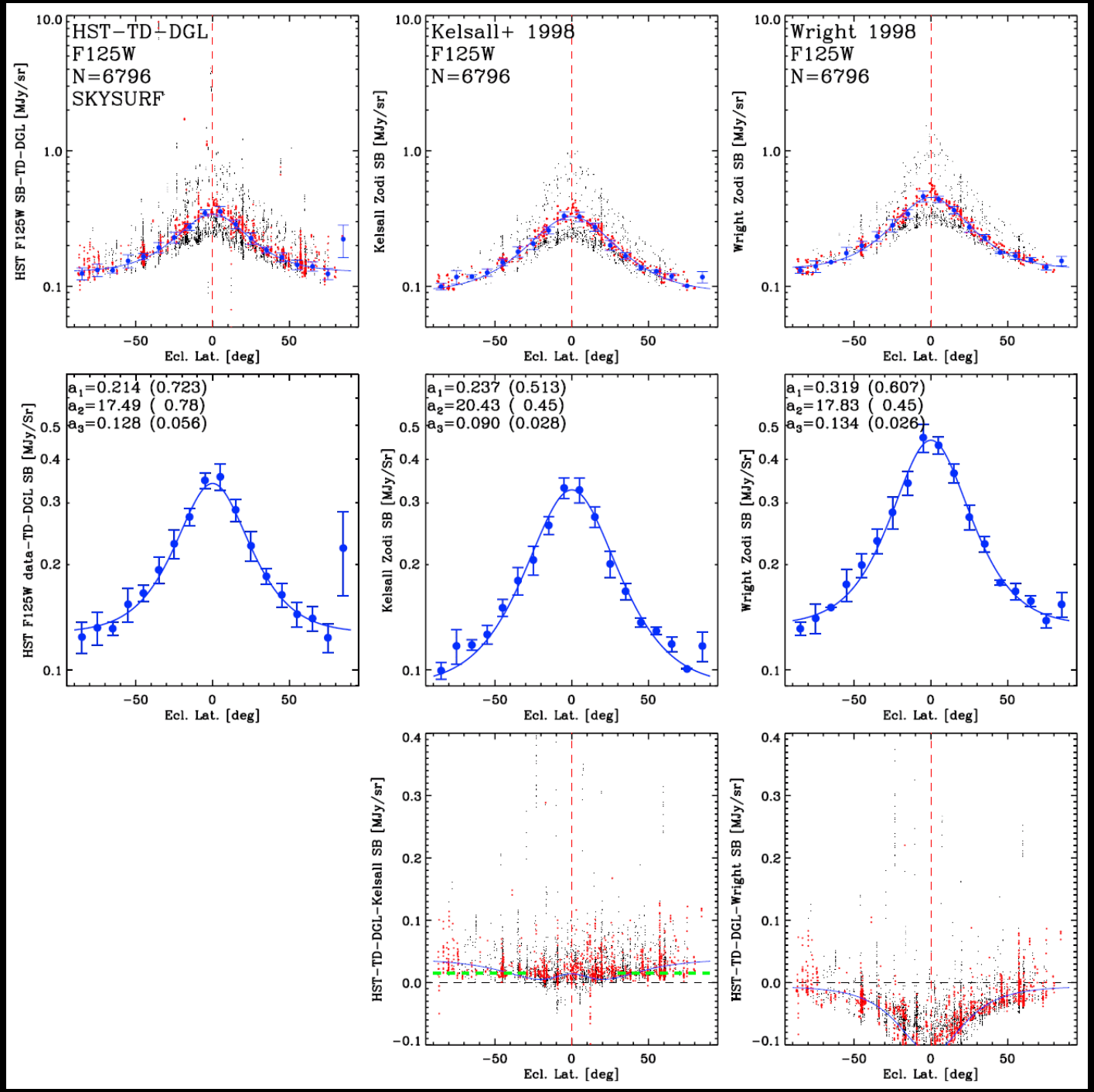

1.25 μm [Left]: HST; [Middle] Kelsall; [Right] Wright model vs. b^{Ecl}.

HST(TD+DGL-subtracted): Kelsall linear offset stays; Wright shows none.

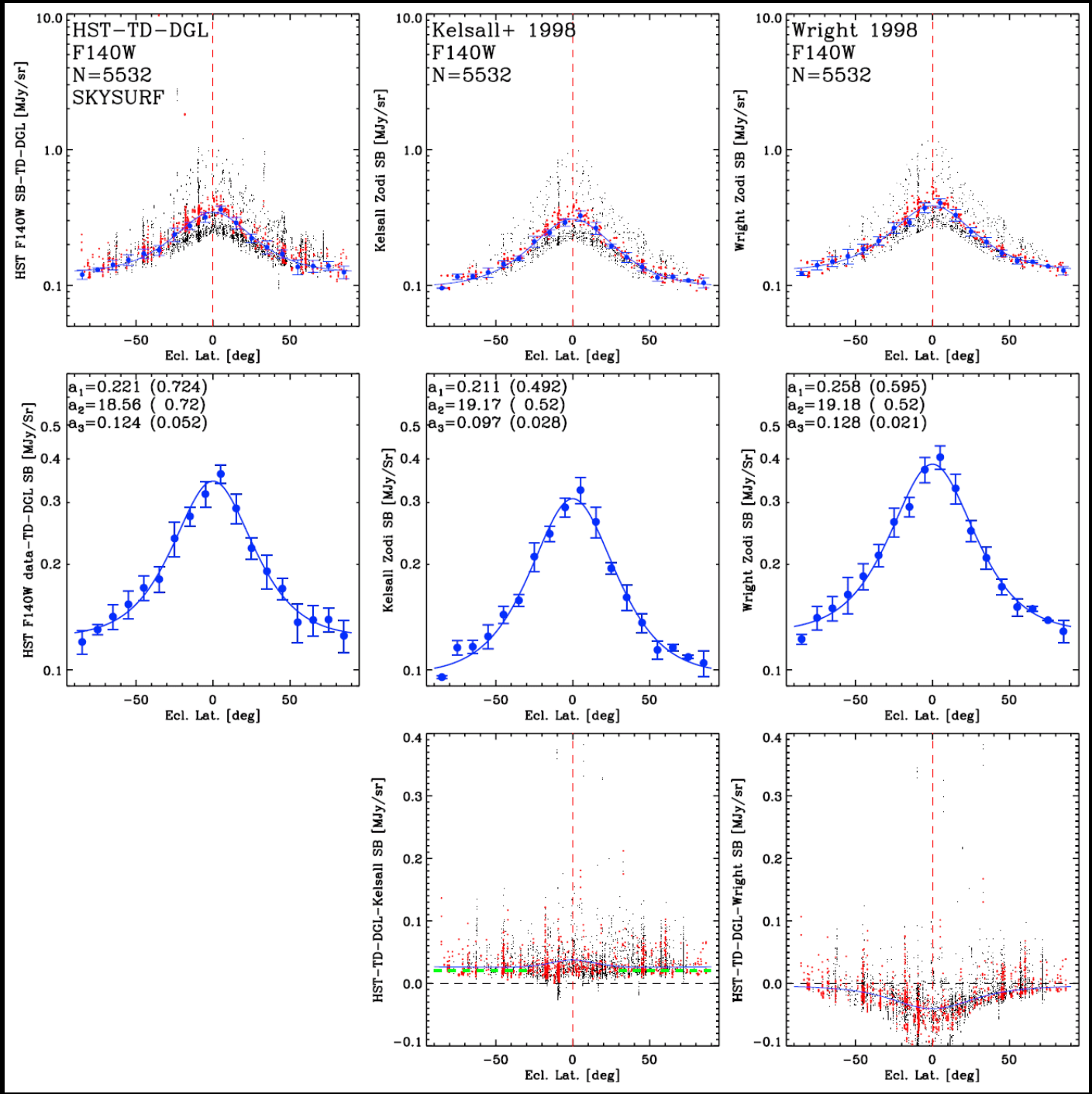

1.40 μm [Left]: HST; [Middle] Kelsall; [Right] Wright model vs. b^{Ecl}.

HST(TD+DGL-subtracted): Kelsall linear offset stays; Wright shows none.

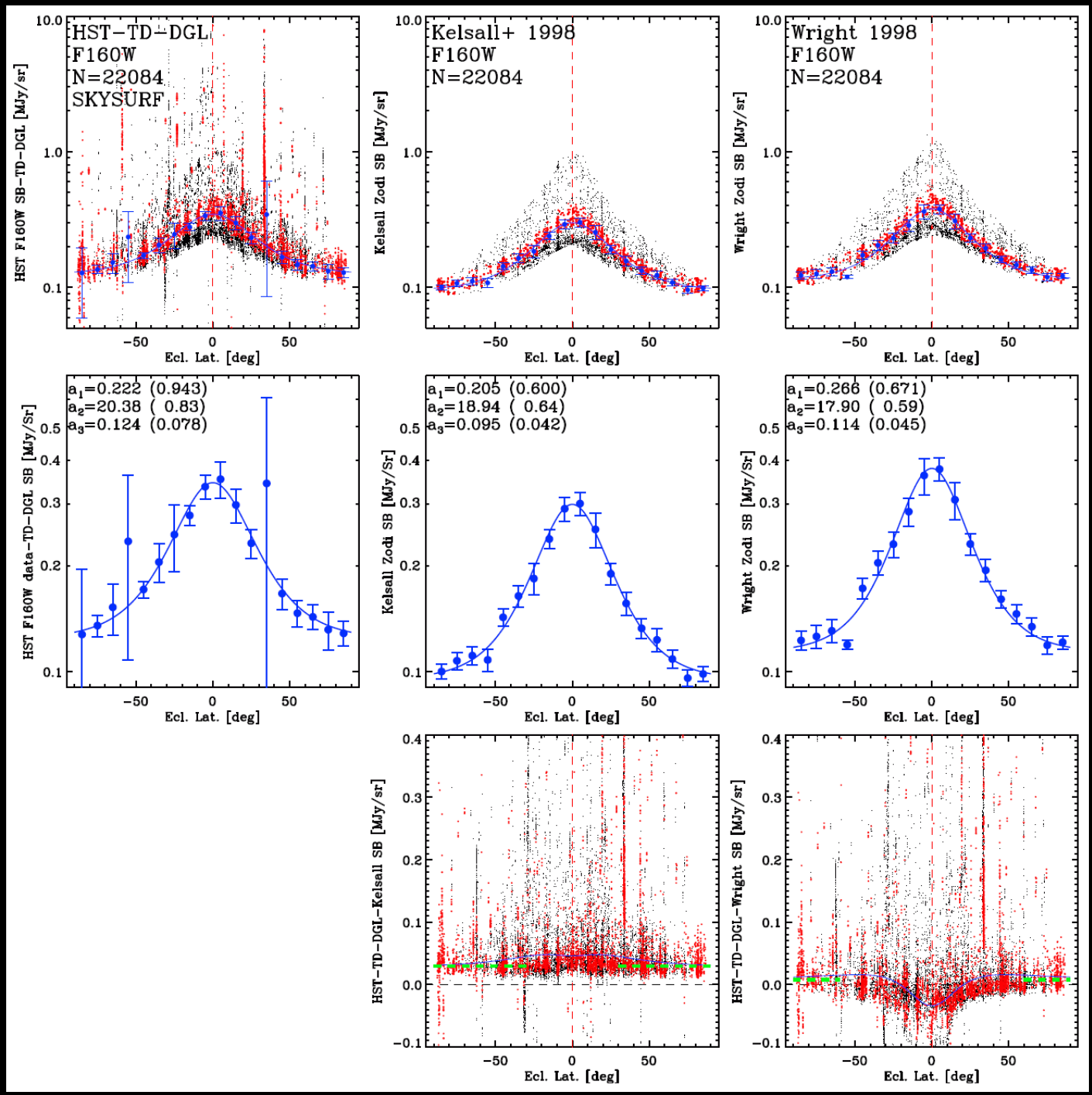

1.60 μm [Left]: HST; [Middle] Kelsall; [Right] Wright model vs. b^{Ecl}.

HST(TD+DGL-subtracted): Kelsall linear offset stays; Wright has marginal.

We must also subtract the HST WFC3/IR Thermal Dark signal:

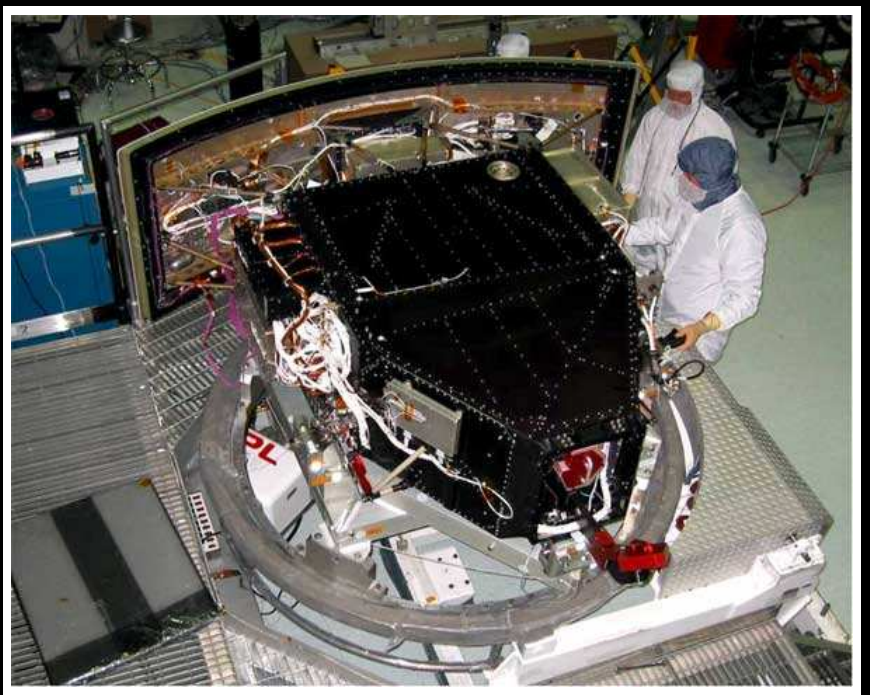

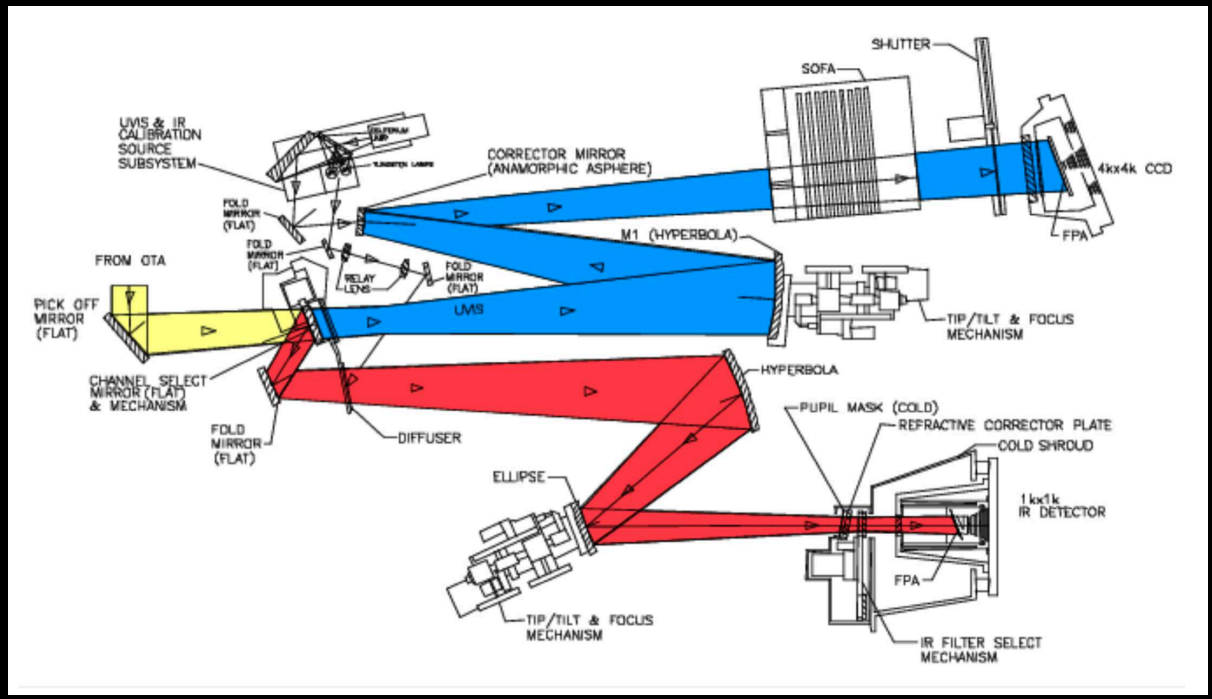

[Left] WFC3 at NASA GSFC before May 2009 Shuttle launch.

[Right] WFC3 model: optical train Temp ranges from T=287–173 K.

• Several dozen temperature sensors monitor temperature T across orbit within 1–2 K, enabling predictions of Thermal Dark (TD) signal vs. T.

• The ***synphot*** package predicts Planck-BB/solid-angle contribution from each optical component vs. T as seen by the WFC3/IR-detector.

(Details in Carleton, T. et al. 2022, AJ, 164, 170; & Carleton, et al. 2023)

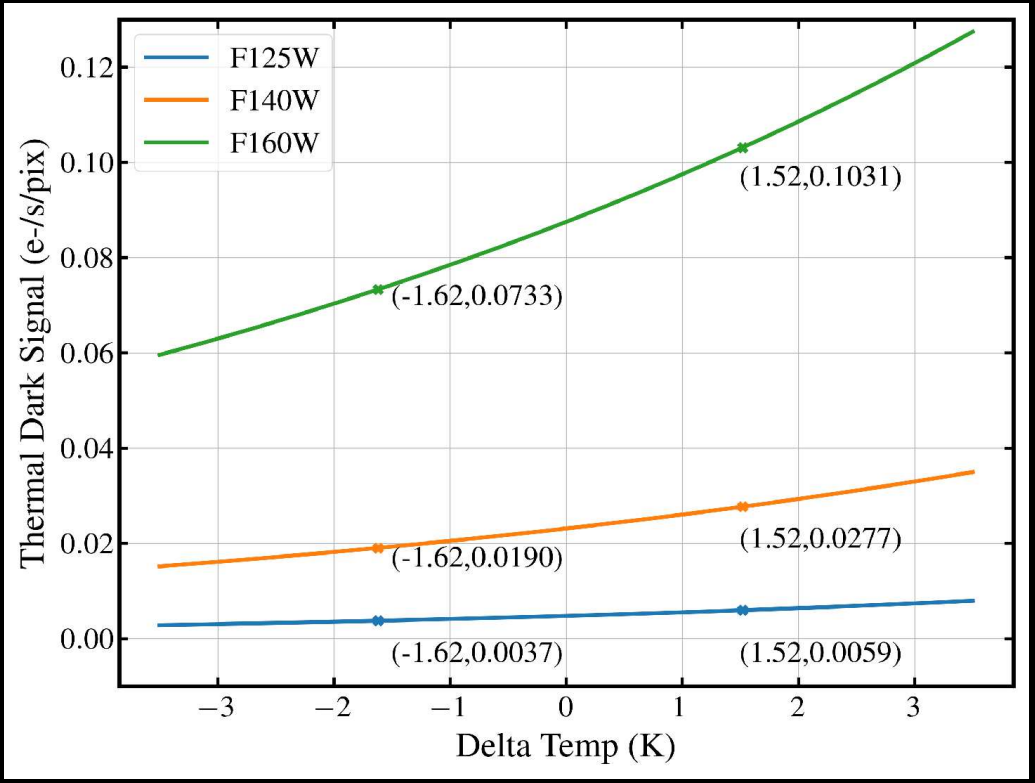

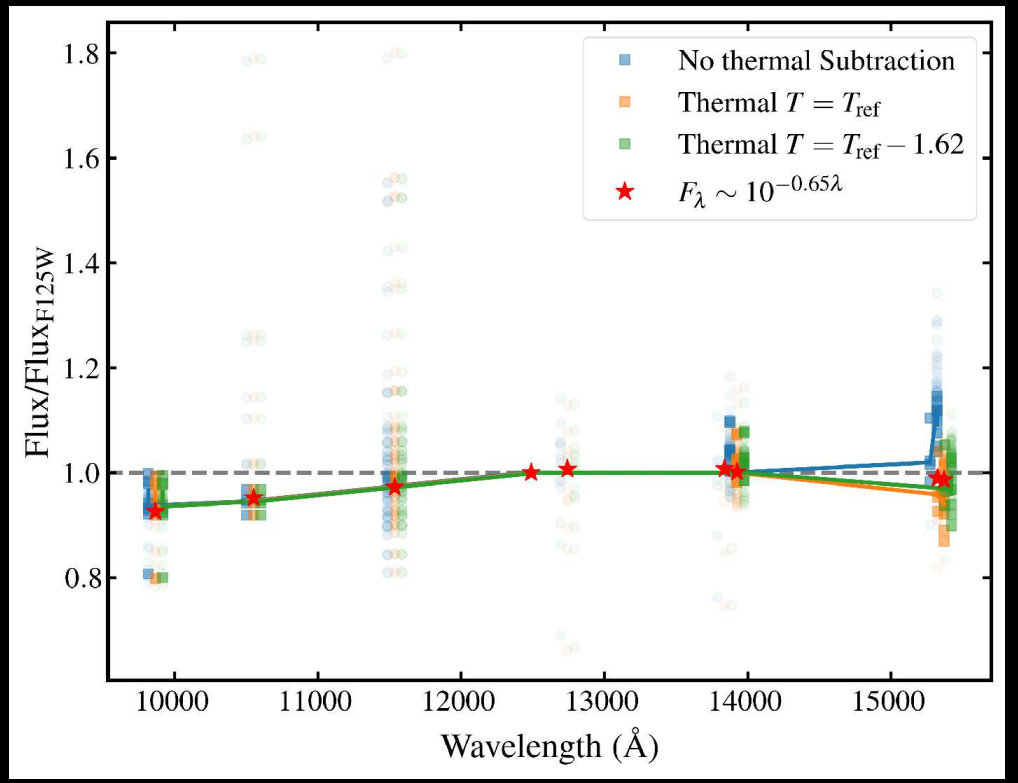

[Left]: ***synphot*** WFC3/IR Thermal Dark (TD) signal modeling.

[Right]: TD for $< \Delta$T(HST)$> \simeq -1.62$ K (compared to nominal T).

- Thermal Dark signal largest at 1.6 μm, but well determined and small at 1.25–1.40 μm (Carleton, McIntyre et al. 2023).

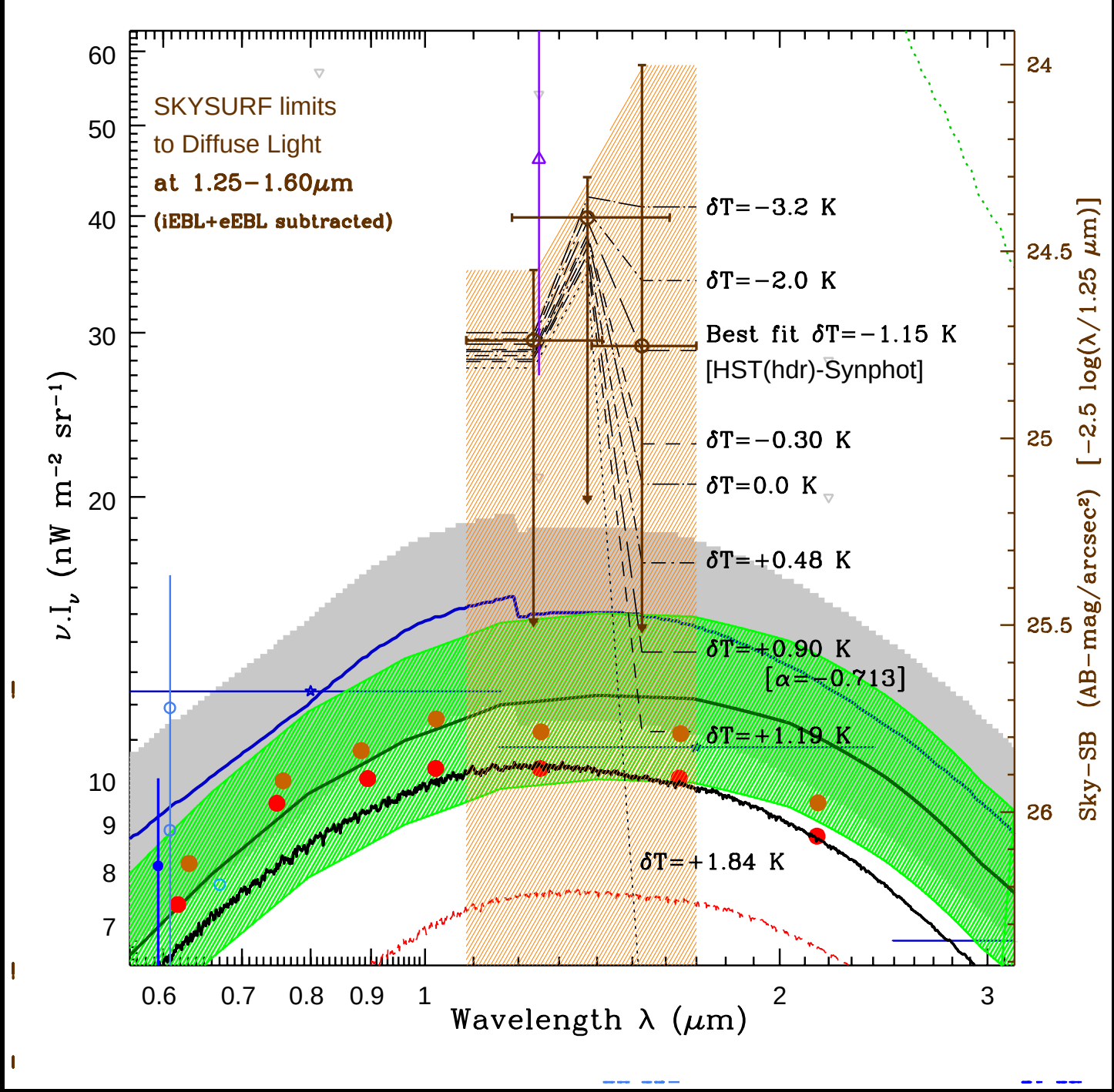

HST shows $\lesssim$29-40 nW/m^2/sr of diffuse light at 1.25-1.6 μm compared to Kelsall's Zodiacal model.

- HST sees no significant signal compared to the Wright model.

- HST diffuse light at 1 AU larger than New Horizon's 8–10 nW/m^2/sr at 43–51 AU (Lauer$^+$ 20, 21).

Next step: Refine Zodiacal models to explain (most/all?) of the diffuse light.

- May need to include higher-albedo Oort Cloud Comet dust at D$\sim$1–3 AU.

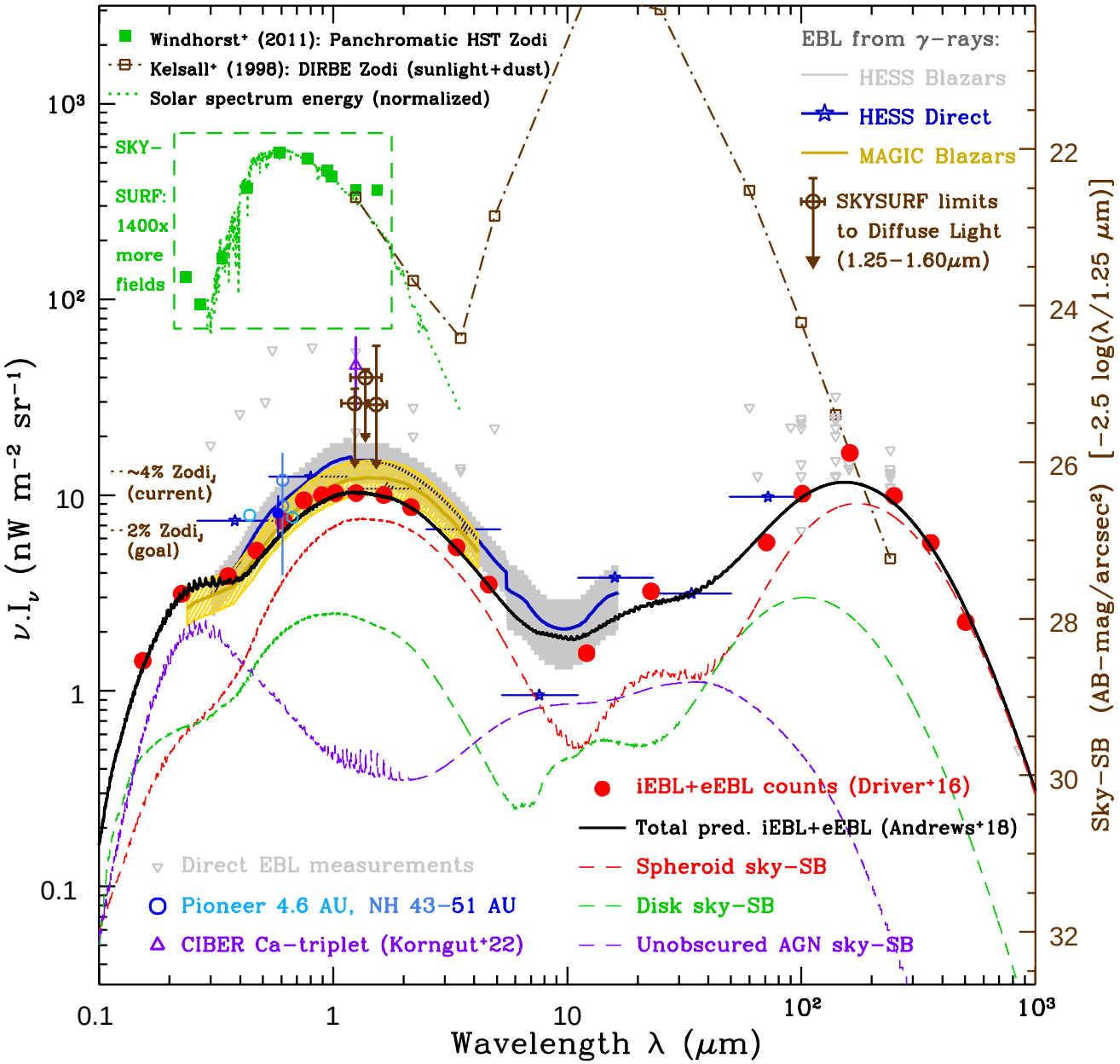

Total Energy vs. λ:

(Driver+ 16; Windhorst+ 18, 21):

Sunlight scattered off the Zodiacal dust.

Thermal radiation from $\gtrsim$240 K Zodiacal dust.

Grey dots: Diffuse EBL from direct experiments.

Dots: Discrete EBL from galaxy counts (+models).

Lauer (2021, 2022) NH at 43-51 AU. SKYSURF 1.25–1.6 μm limits.

At 1 AU, SKYSURF sees $\lesssim$29–40 nW/m^2/sr of diffuse 1.25–1.6 μm light!

(Carleton, T. et al. 2022, AJ, 164, 170; Windhorst, R. et al. 2022, AJ, 164, 14; — 2023, AJ, 165, 13).

(2) JWST Constraints to Diffuse Light from the PEARLS Project

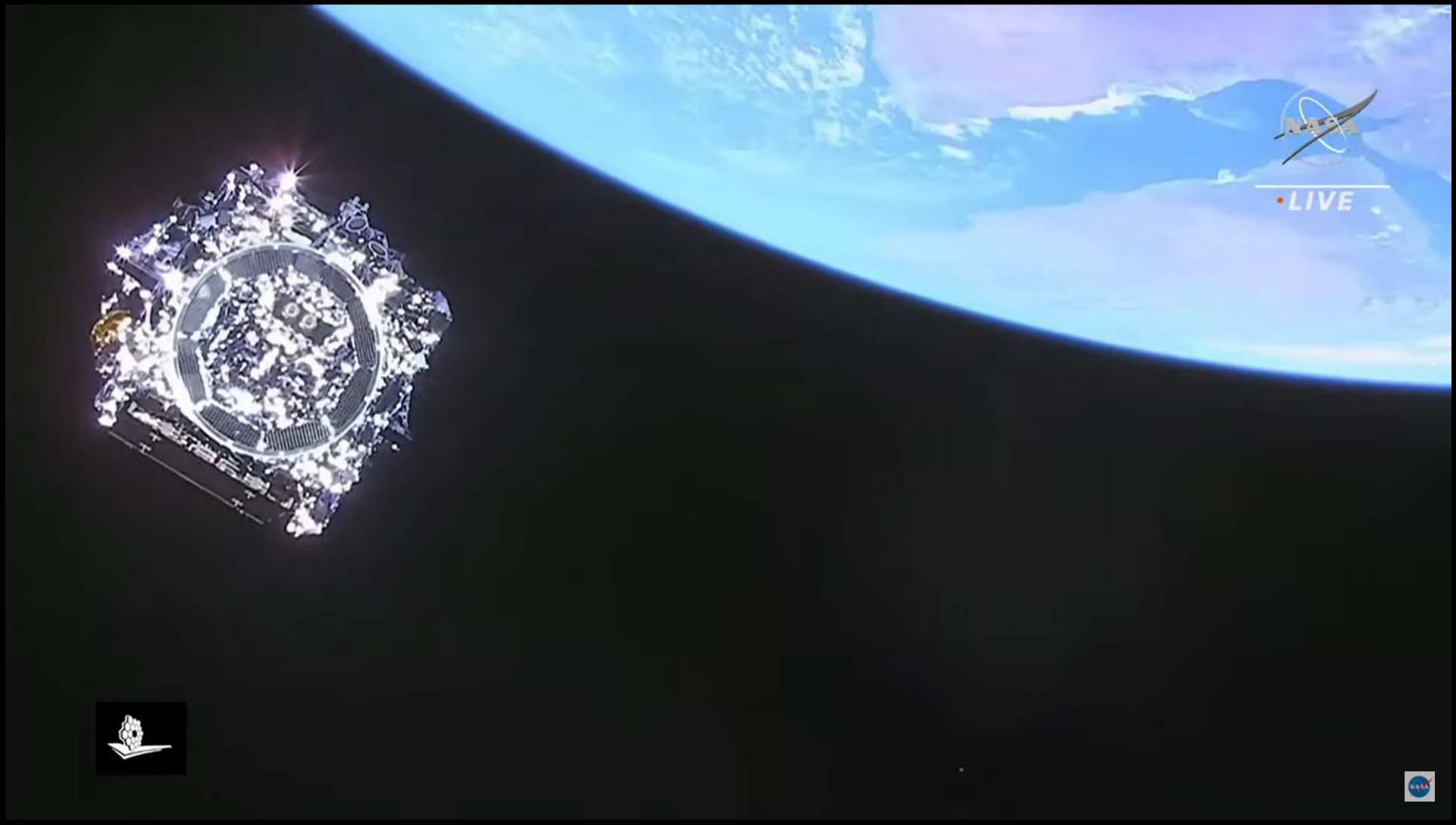

What Diffuse Light limits can JWST set from the ultradark L2 environment?

- HST has had 180,500 sunrises + sunsets since its April 1990 launch;
- JWST has had only 1 sunrise + 1 sunset since its Dec. 2021 launch!

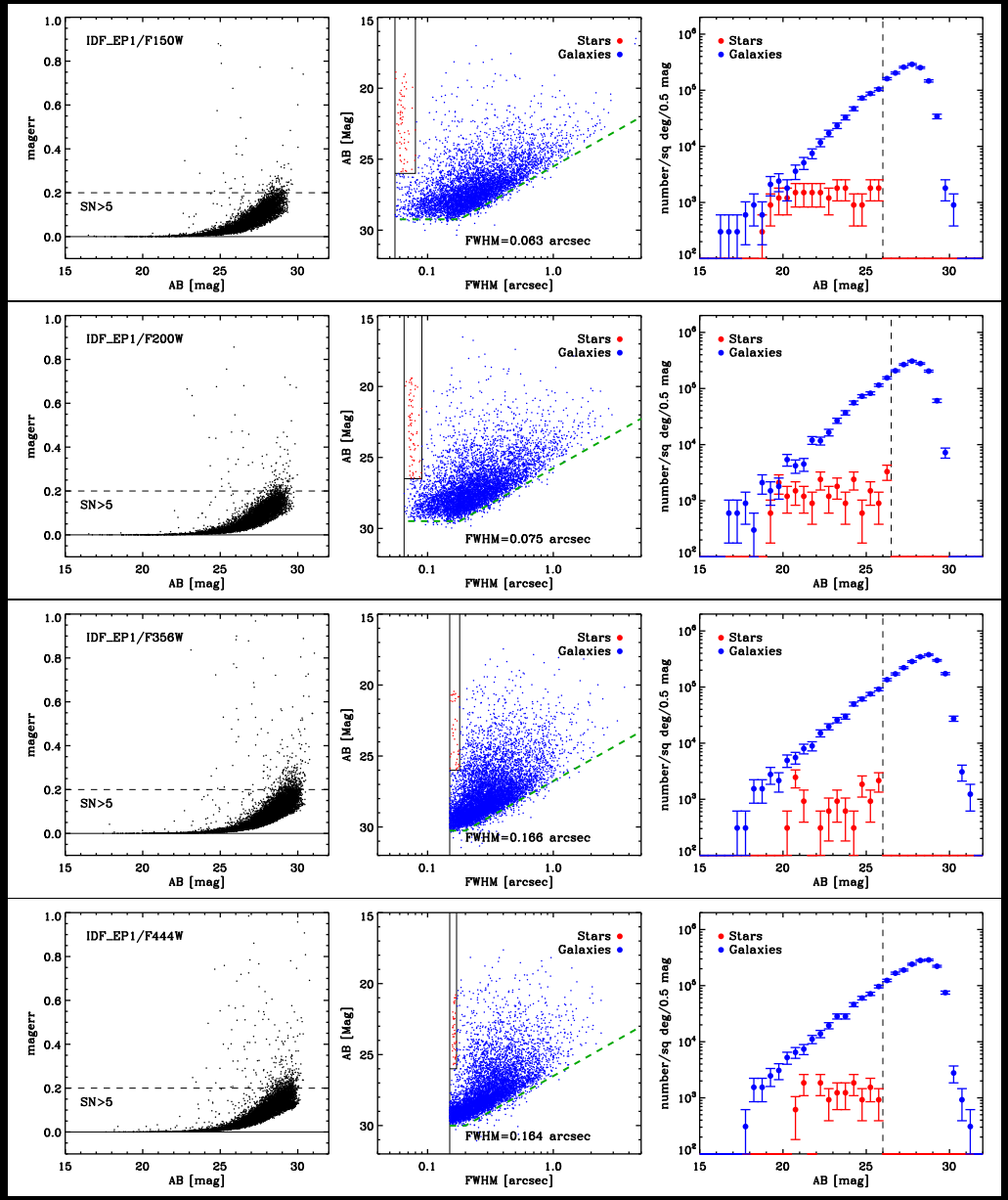

[Left]: Mag-error vs. AB: 5σ NIRCam completeness to AB$\lesssim$28.5–29 mag.

[Middle]: AB vs. FWHM: accurate star-galaxy separation to AB$\lesssim$26-27!

- Stellar sequence FWHM improves below 2.00 μm JWST diffraction limit!

[Right]: 0.9–4.5μm Galaxy counts complete to AB$\lesssim$28.5–29 mag, resp.

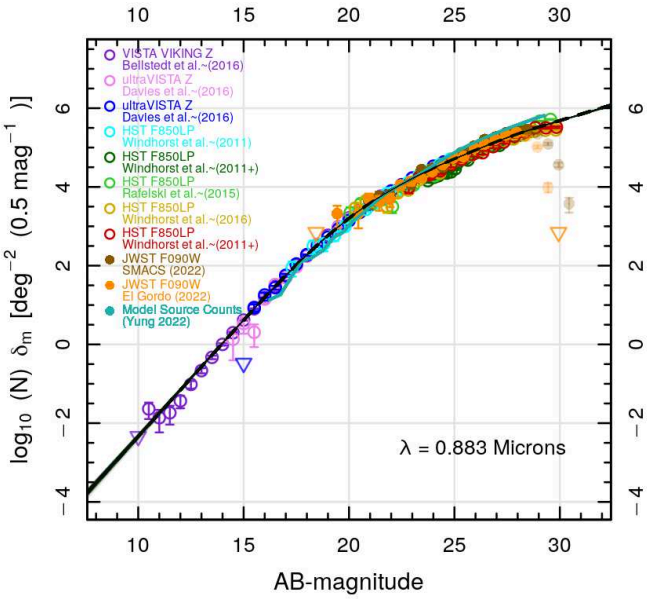

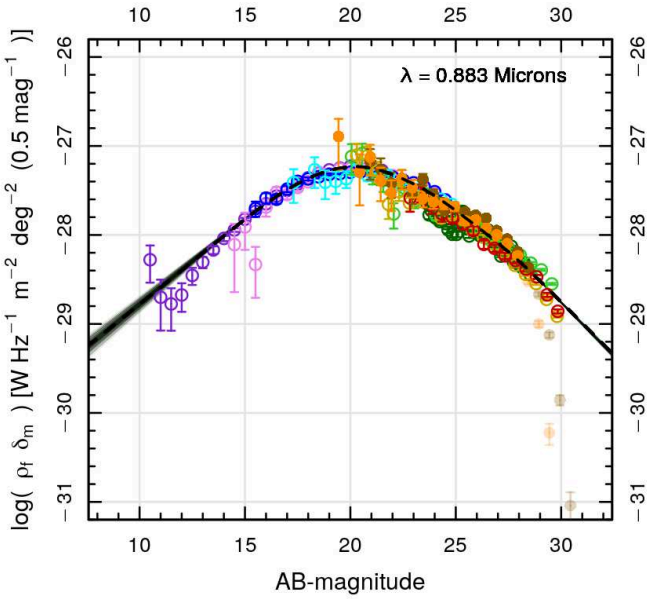

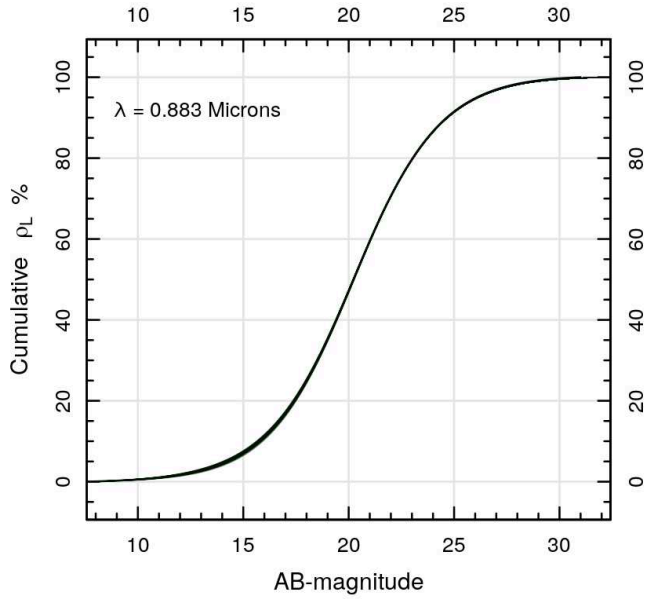

[Left]: Normalized differential galaxy counts.

[Middle]: Galaxy energy counts (after dividing by 0.4 dex/mag slope).

[Right]: Integrated Galaxy Light (IGL) from best fit spline.

0.88 μm Ground-based+HST+JWST galaxy counts (AB$\simeq$10–30 mag).

- Energy counts narrow with increasing λ. Peak amplitude around 2 μm.

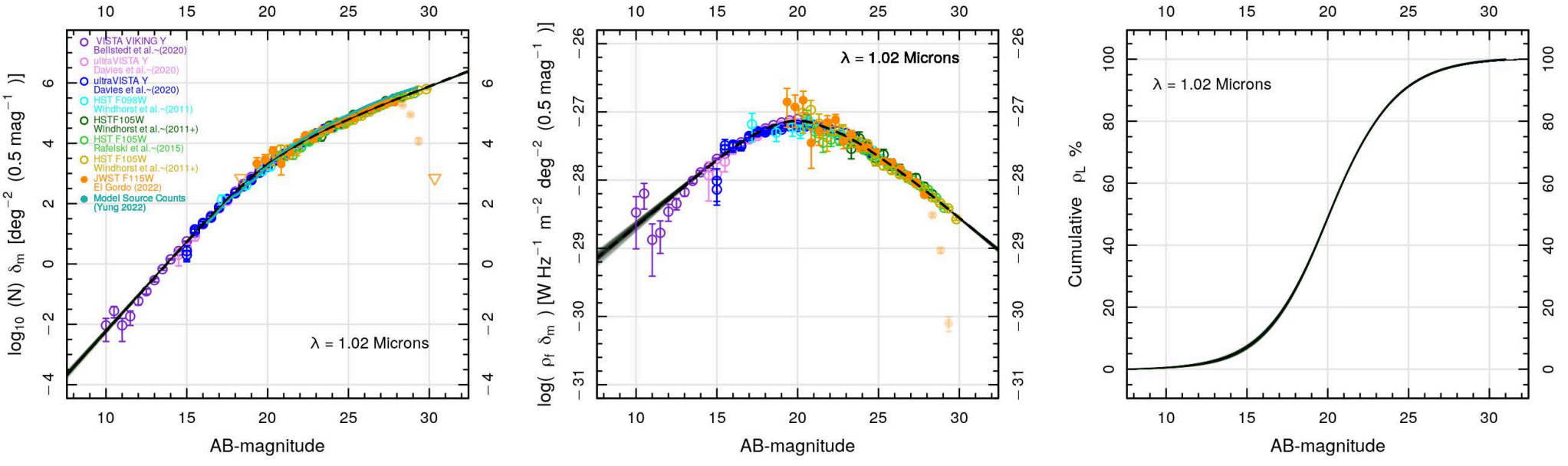

[Left]: Normalized differential galaxy counts.

[Middle]: Galaxy energy counts (after dividing by 0.4 dex/mag slope).

[Right]: Integrated Galaxy Light (IGL) from best fit spline.

1.02 μm Ground-based+HST+JWST galaxy counts (AB$\simeq$10–30 mag).

- Energy counts narrow with increasing λ. Peak amplitude around 2 μm.

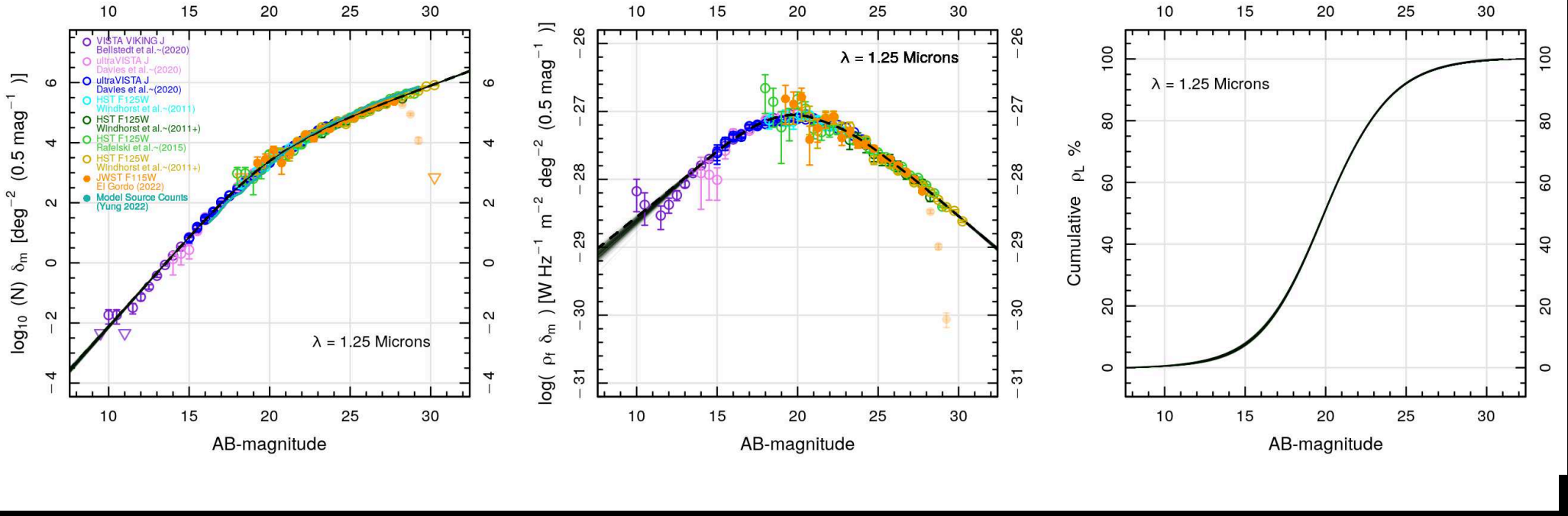

[Left]: Normalized differential galaxy counts.

[Middle]: Galaxy energy counts (after dividing by 0.4 dex/mag slope).

[Right]: Integrated Galaxy Light (IGL) from best fit spline.

1.25 μm Ground-based+HST+JWST galaxy counts (AB$\simeq$10–30 mag).

- Energy counts narrow with increasing λ. Peak amplitude around 2 μm.

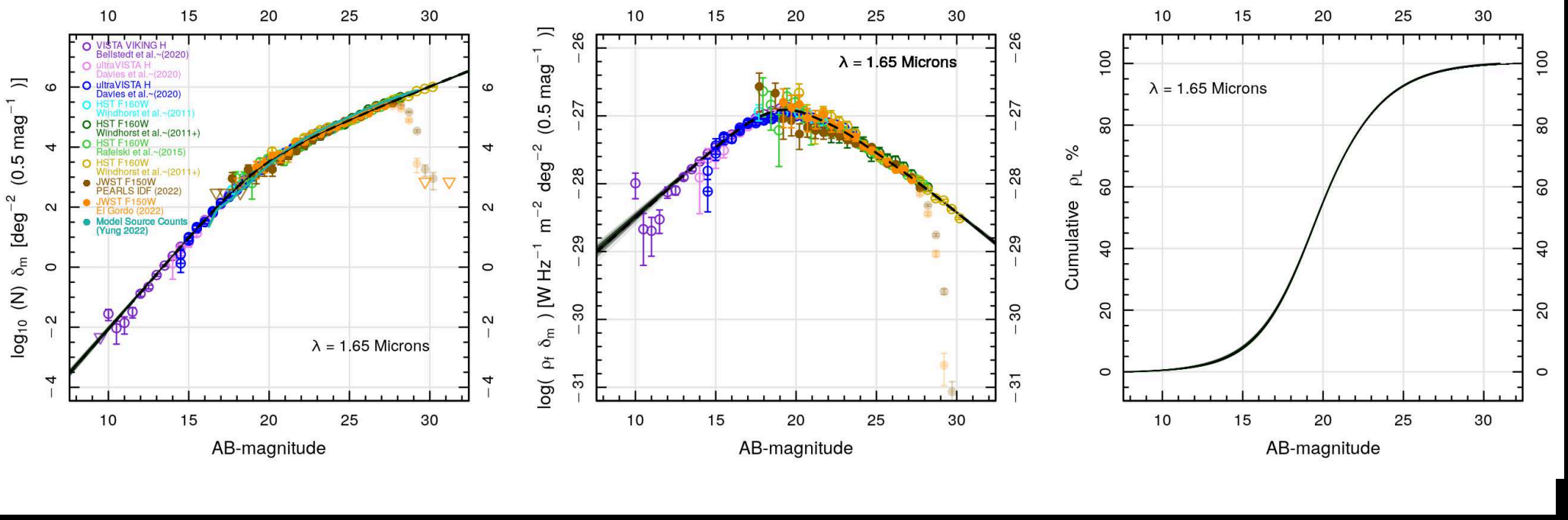

[Left]: Normalized differential galaxy counts.

[Middle]: Galaxy energy counts (after dividing by 0.4 dex/mag slope).

[Right]: Integrated Galaxy Light (IGL) from best fit spline.

1.65 μm Ground-based+HST+JWST galaxy counts (AB$\simeq$10–30 mag).

- Energy counts narrow with increasing λ. Peak amplitude around 2 μm.

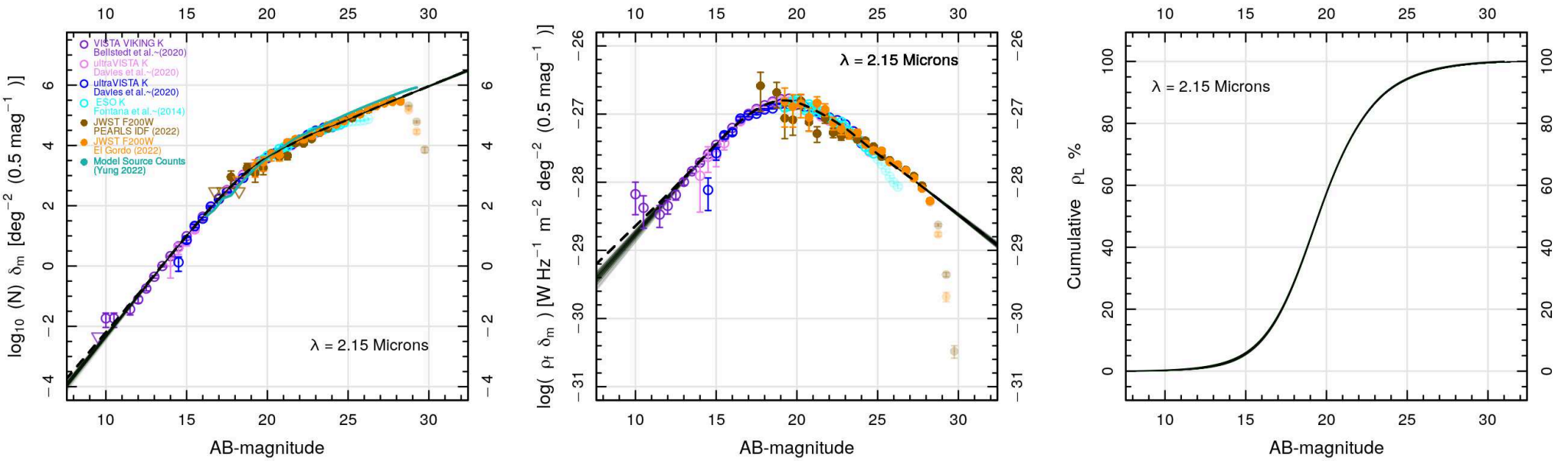

[Left]: Normalized differential galaxy counts.

[Middle]: Galaxy energy counts (after dividing by 0.4 dex/mag slope).

[Right]: Integrated Galaxy Light (IGL) from best fit spline.

2.15 μm Ground-based+JWST galaxy counts (AB$\simeq$10–30 mag).

- Energy counts narrow with increasing λ. Peak amplitude around 2 μm.

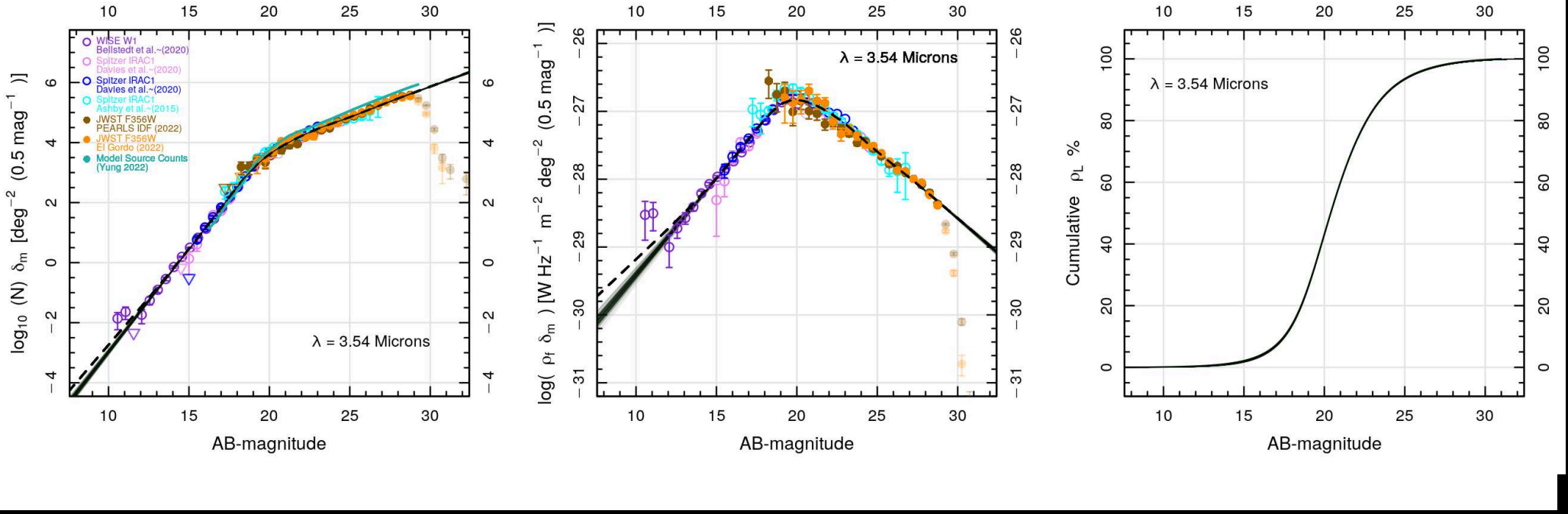

[Left]: Normalized differential galaxy counts.

[Middle]: Galaxy energy counts (after dividing by 0.4 dex/mag slope).

[Right]: Integrated Galaxy Light (IGL) from best fit spline.

3.54 μm WISE+Spitzer+JWST galaxy counts (AB$\simeq$10–30 mag).

- Energy counts narrow with increasing λ. Peak amplitude around 2 μm.

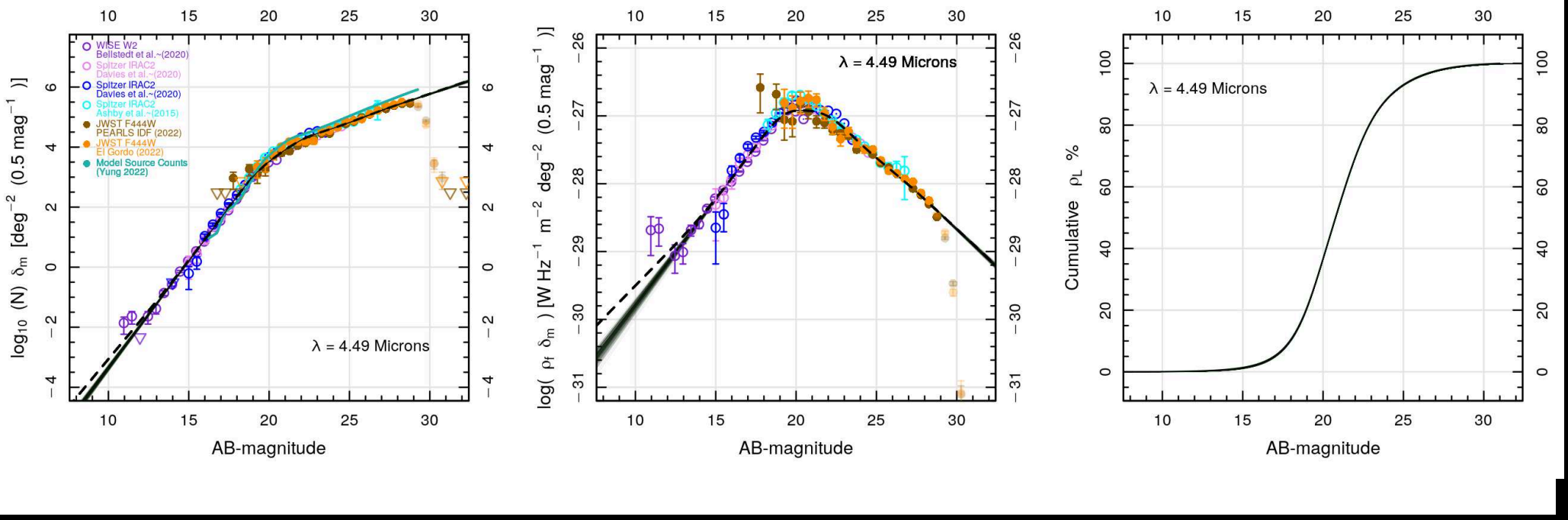

[Left]: Normalized differential galaxy counts.

[Middle]: Galaxy energy counts (after dividing by 0.4 dex/mag slope).

[Right]: Integrated Galaxy Light (IGL) from best fit spline.

4.49 μm WISE+Spitzer+JWST galaxy counts (AB$\simeq$10–30 mag).

- Energy counts narrow with increasing λ. Peak amplitude around 2 μm.
- 0.9–4.5 μm Integrated Galaxy Light (IGL) now well determined ($\lesssim$10%)!

(Figures by Scott Tompkins; see also Tompkins et al. 2023, MNRAS, 521, 332; astro-ph/2301.03699).

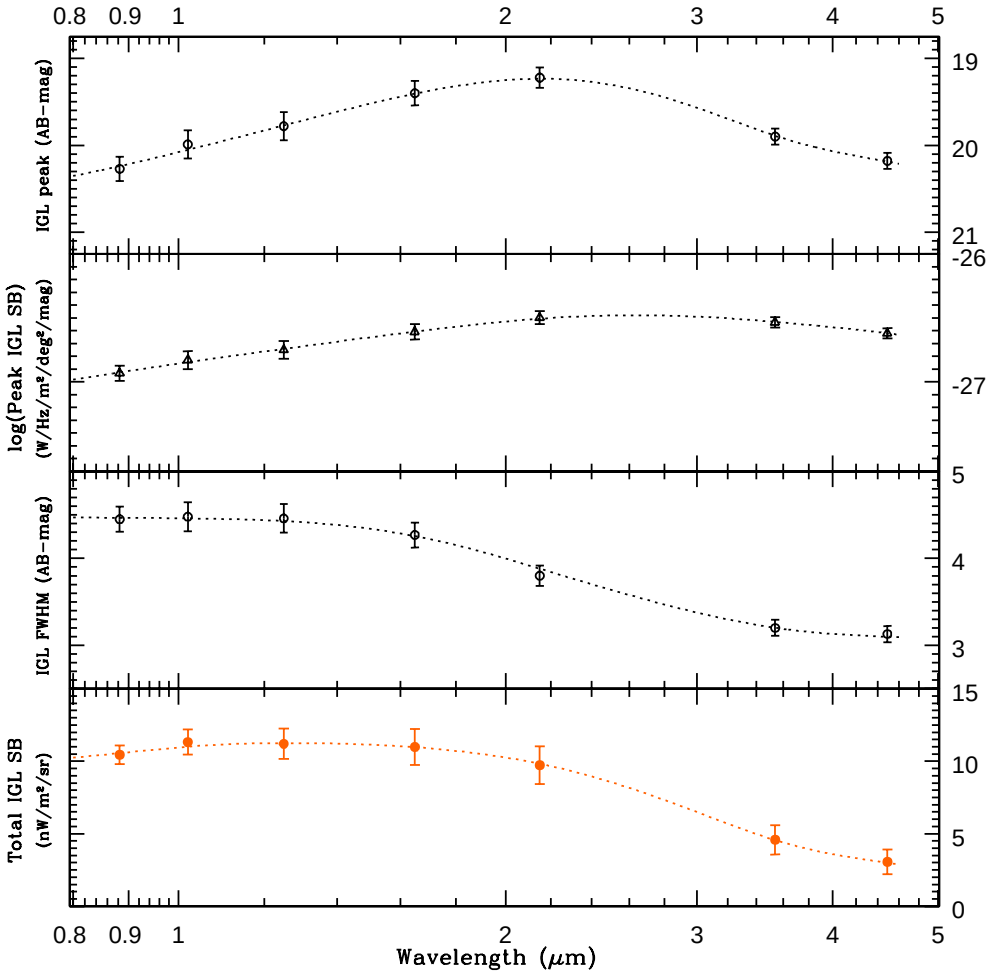

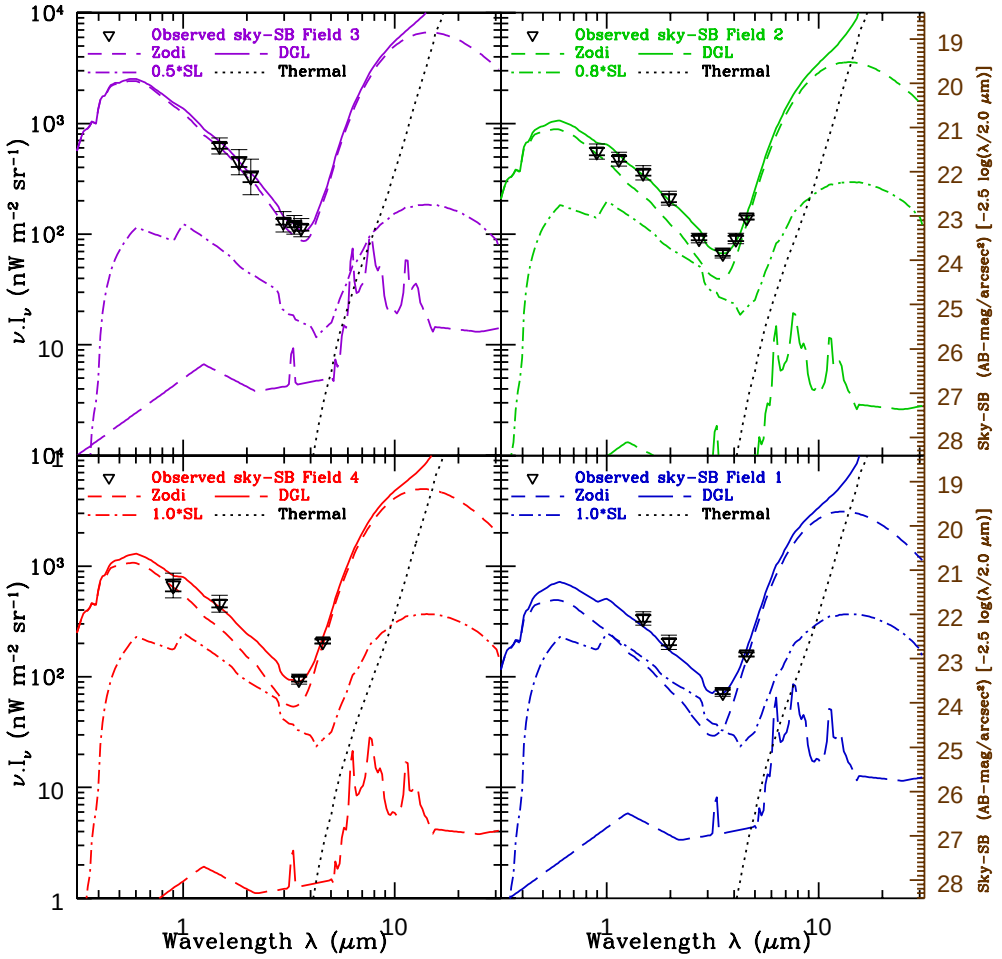

[Left]: IGL vs. λ: Peak (AB & mks units); IGL FWHM (AB); and $\nu.I_\nu$.

- 0.9–4.5 μm Integrated Galaxy Light (IGL) now well determined ($\lesssim$10%)!

[Right]: 13-band sky-SB vs. λ: Model-sum = Zodi + JWST-Straylight (SL) + Diffuse Galactic Light (DGL) + JWST Thermal Radiation

- Model-sums match total JWST NIRCam sky-SB within $\sim$10% of Zodi.

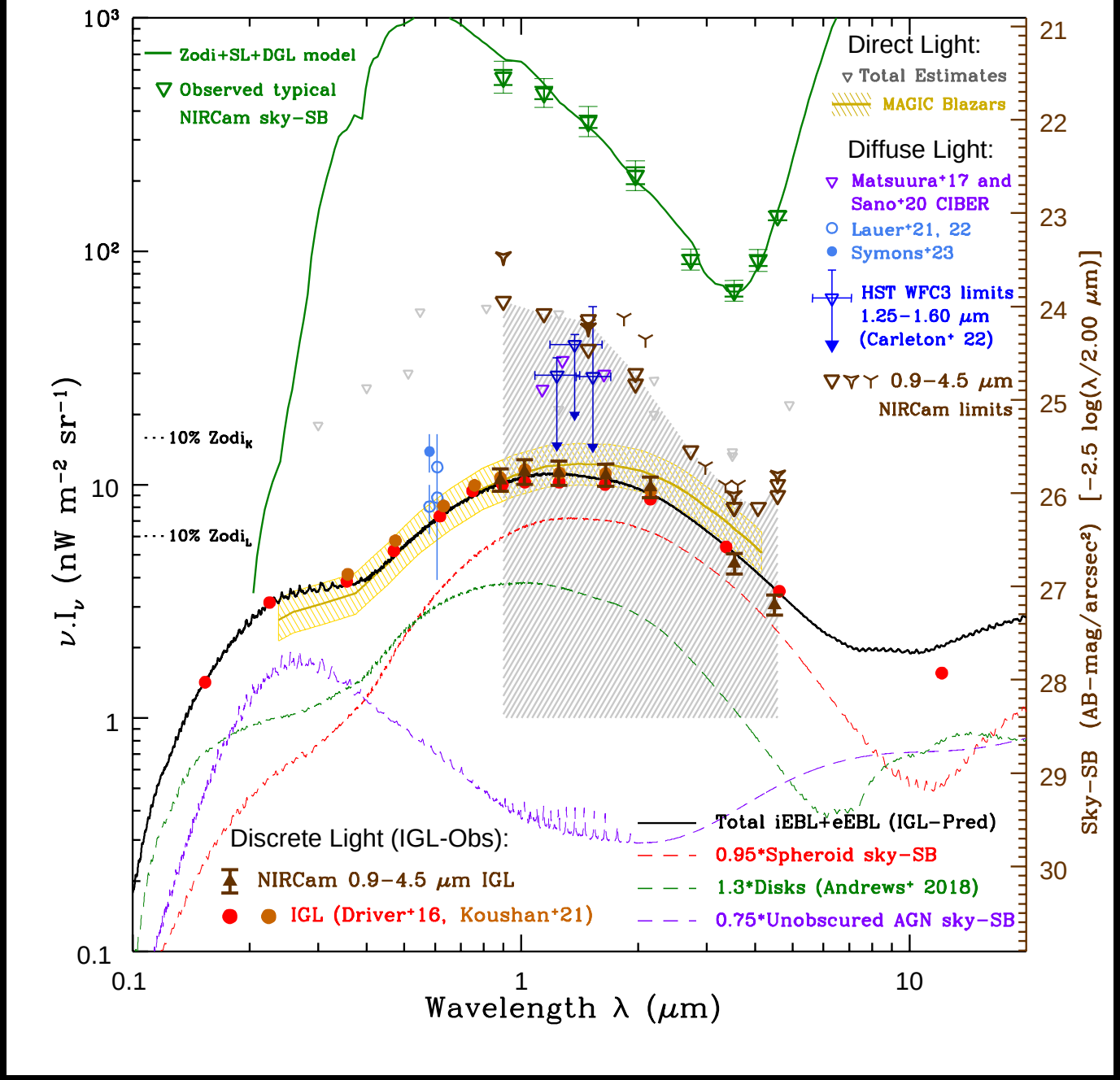

Conclusions: (1) JWST NIRCam accurately determined 0.9-4.5 μm IGL.
(2) 0.9-2μm diffuse light limits confirm previous work. Firm 2.7-4.5μm limits.

- 3–5 μm limits ($\lesssim$8 nW/m^2/sr) to improve with many more JWST fields.

(3) Summary and Conclusions

(1) HST built to measure faint objects & sky over decades at 0.2-1.6 μm.

(2) More than 95% of photons in STScI Archive come from D$\lesssim$3–5 AU.

Traditional imaging techniques ignored sky-foreground for 28 years.

(3) SKYSURF can measure sky-SB to $\lesssim$3–4% & identify orbital straylight.

(4) Compared to Kelsall et al.'s (1998) Zodiacal model, SKYSURF finds $\lesssim$29–40 nW/m^2/sr ($\sim$7% of Zodi) of diffuse light at 1.25–1.6 μm.

- This amounts to the *brightness* of $\sim$10 Jupiters over 4π steradian!
- Compared to Wright's (1998) Zodiacal model, HST finds no significant diffuse light at 1.25–1.6 μm.

(5) JWST yields best limits of $\lesssim$8 nW/m^2/sr in its darkest 3-5 μm sky.

(6) Zodiacal models need update to include dim spherical diffuse light.

- Need to include higher-albedo Oort Cloud Comet dust at D$\sim$1–3 AU?

SPARE CHARTS

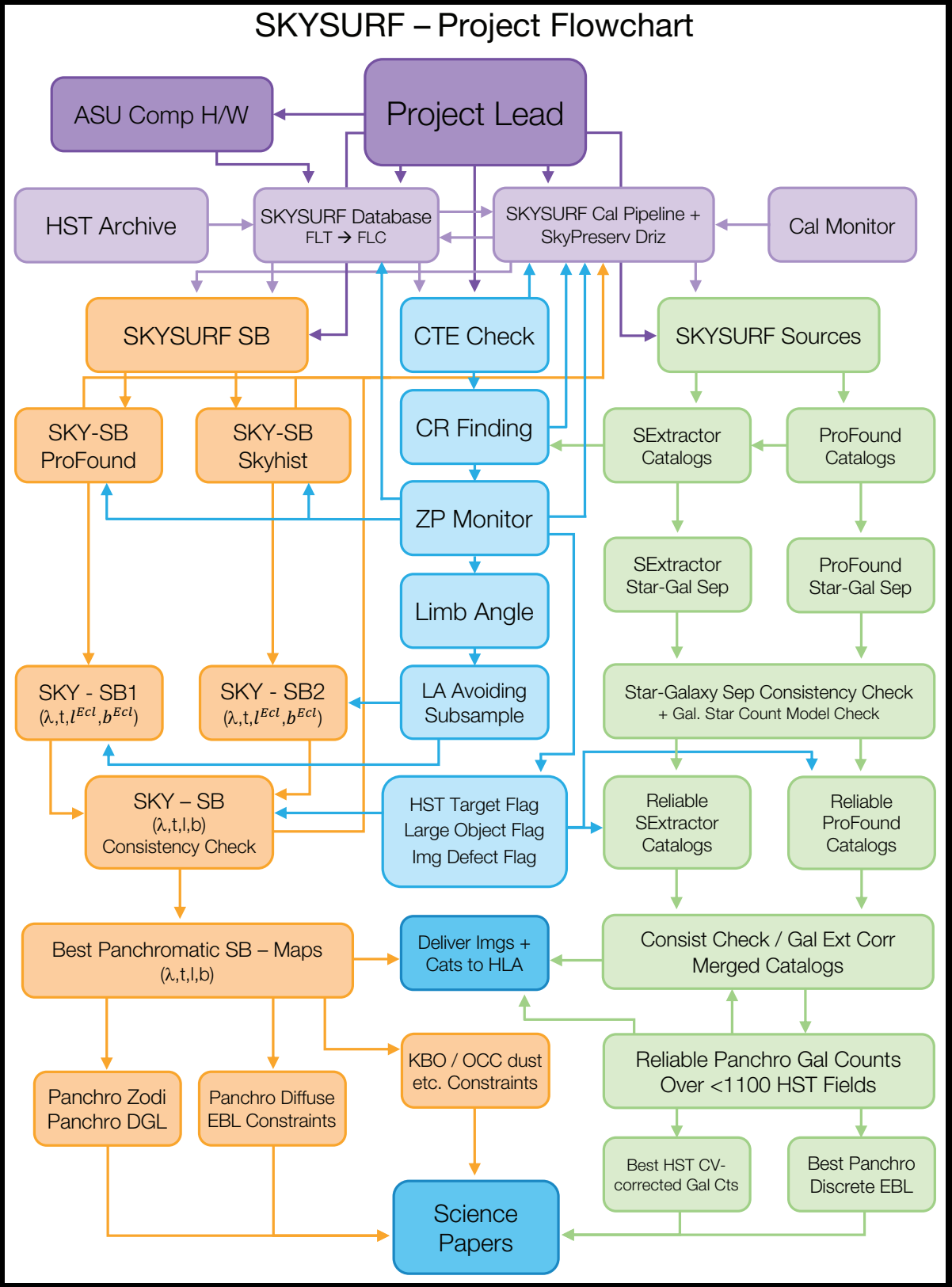

Measuring sky foreground & making object catalogs:

SKYSURF project flowchart:

Database building and standard pipeline

Monitor systematics: Cosmic Ray filter, CTE-correction, Zeropoints, orbital straylight, artifact flagging & removal.

sky-SB estimates with two independent algorithms.

Object finding/catalogs with two independent algorithms.

Table 5. Error Estimates[a] in Calibration, Zeropoints, Sky-SB Measurements, and Thermal Dark Signals

Source of Error	WFPC2	ACS/WFC	WFC3/UVIS	— WFC3/IR —			(§§)
				F125W	F140W	F160W	
(1)	(2)	(3)	(4)	(5)	(6)	(7)	(8)
Bias/Darkframe subtraction	∼1.0%	∼1.5%	∼1.5%	∼1.0%	∼1.0%	∼1.0%	4.1
Dark glow subtraction	∼2%	—	—	—	—	—	4.1.1
Postflash subtraction	—	∼1%	∼1%	—	—	—	4.1
Global flat-field quality[b]	∼1–3%	0.6–2.2%	∼2–3%	∼0.5–2%	∼0.5–2%	∼0.5–2%	4.1
Numerical accuracy of LES[c]	≲0.1–0.4%	≲0.1–0.4%	≲0.1–0.4%	≲0.1–0.4%	≲0.1–0.4%	≲0.1–0.4%	4.2.3
Photometric zeropoints[d]	∼2%	0.5–1%	0.5–1%	∼1.5%	∼1.5%	∼1.5%	4.1.5
Thermal Dark signal[e]	—	—	—	∼1%	∼1%	∼3%	4.1.4, 5.2
Total Error[f]	∼4.3%	∼3.0%	∼3.7%	∼2.9%	∼2.9%	∼4.1%	

[a] *All relative errors* in this table are expressed as a percentage of the typical Zodiacal sky-SB in the F125W, F140W, and F160W filters, which are ∼331, ∼282, ∼240 nW m^{-2} sr^{-1}, respectively (*e.g.*, Fig. 1).

[b] For WFPC2, the large-scale flat-field errors in the filters F439W and redwards are ≲1%, but the upper bound includes the 1% error in the contamination correction and the ∼3% error in the residual CTE correction. For the less frequently used WFPC2 UV filters, these errors can be larger.

[c] Numerical accuracy of Lowest Estimated Sky values away from detected objects (§ 4.2). The LES algorithms also avoid areas of significant persistence or cross-talk when estimating the sky-SB, so these effects are not included as an extra term in the error budget.

[d] For WFC3/IR, this includes the ∼0.5% uncertainty in the applied detector count-rate non-linearity correction (§ 4.1.4).

[e] The errors in the estimated Thermal Dark signal values are given for the F125W and F140W filters as a percentage of the typical Zodiacal sky-SB, and are larger for the F160W filter (§ 5.2).

Absolute HST sky-SB photometry errors ≲3–4% (as fraction of Zodi).

(Windhorst, R. et al. 2023, AJ, 165, 13; Carleton, T. et al. 2022, AJ, 164, 170).

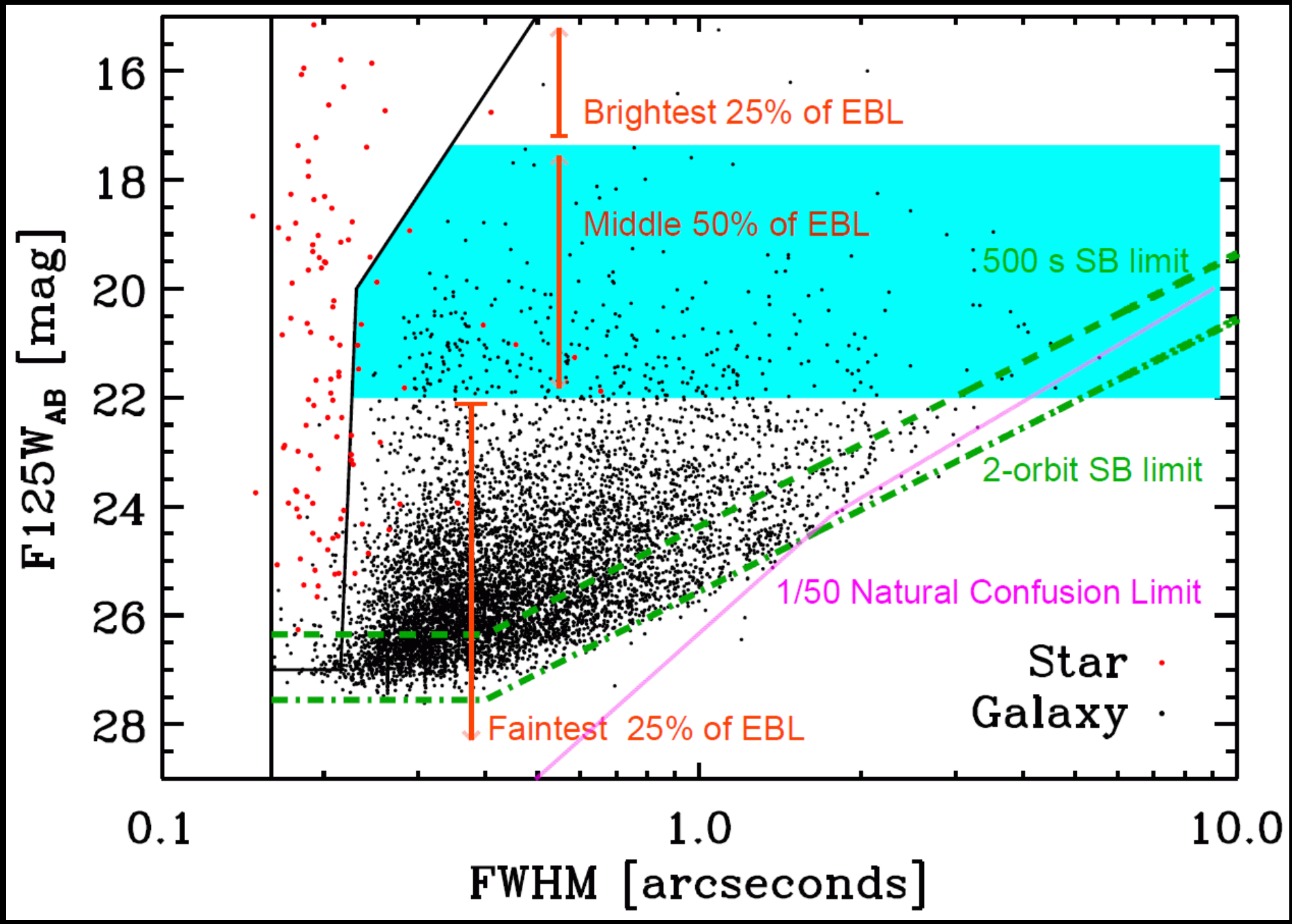

Cohen: star-galaxy separation, with SB- and natural confusion limits.

- Subset of deeper exposures yield accurate completeness corrections.

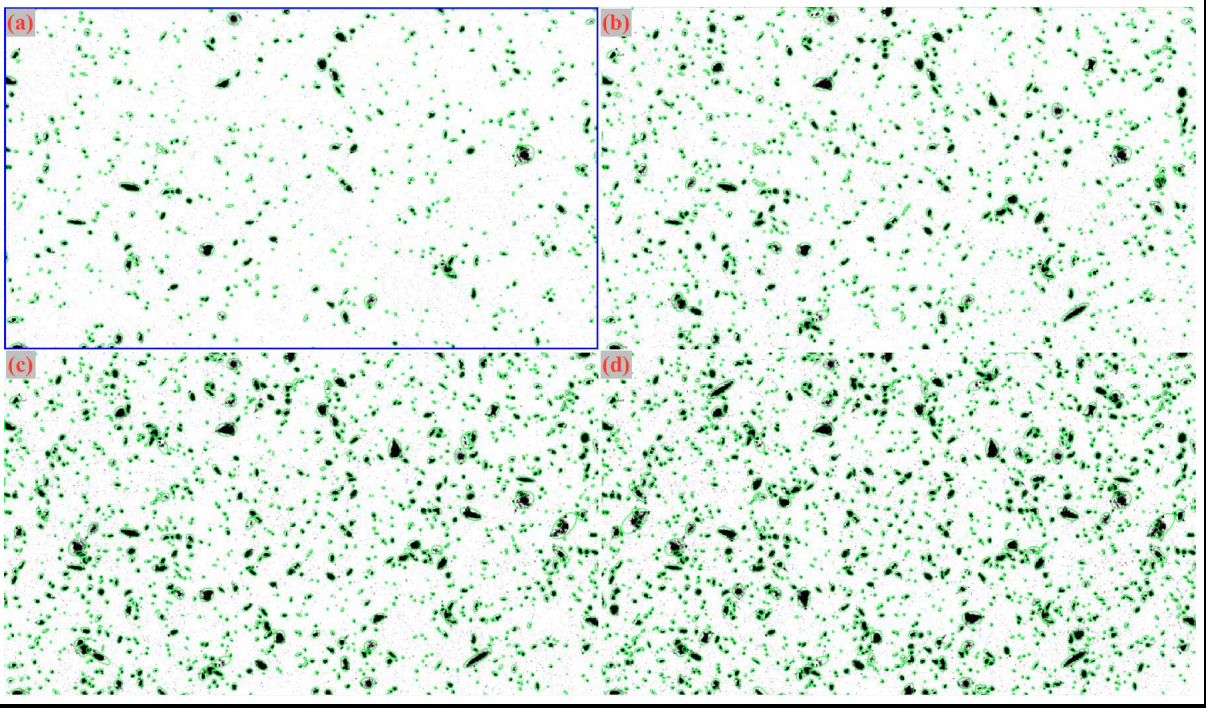

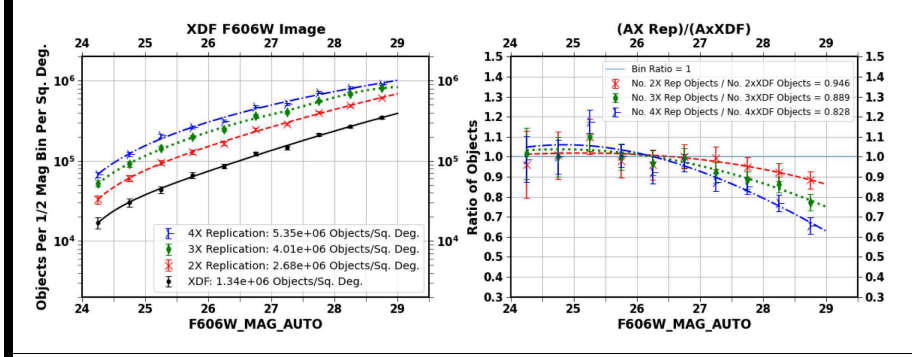

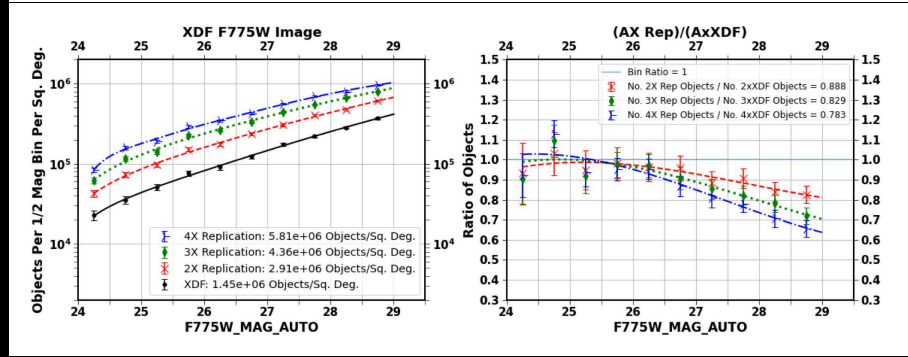

Kramer et al. (2022): Can we really hide a factor $\sim$2–4 of faint galaxies?

[Left]: Add HUDF image to itself 2×, 3×, 4× after n×90° rotation:

[Right]: 4×HUDF counts still $\gtrsim$65% complete for AB$\gtrsim$28.5–29 mag.

- Crowding not enough to explain factor 2–3 diffuse flux at AB$\gtrsim$24 mag.

$\Longrightarrow$ Cannot explain diffuse light through missing ordinary galaxies!

- Missing diffuse light caused by other sources?!

(Kramer, D. et al. 2022, ApJL, 940, L15; astro-ph/2208.07218v2)

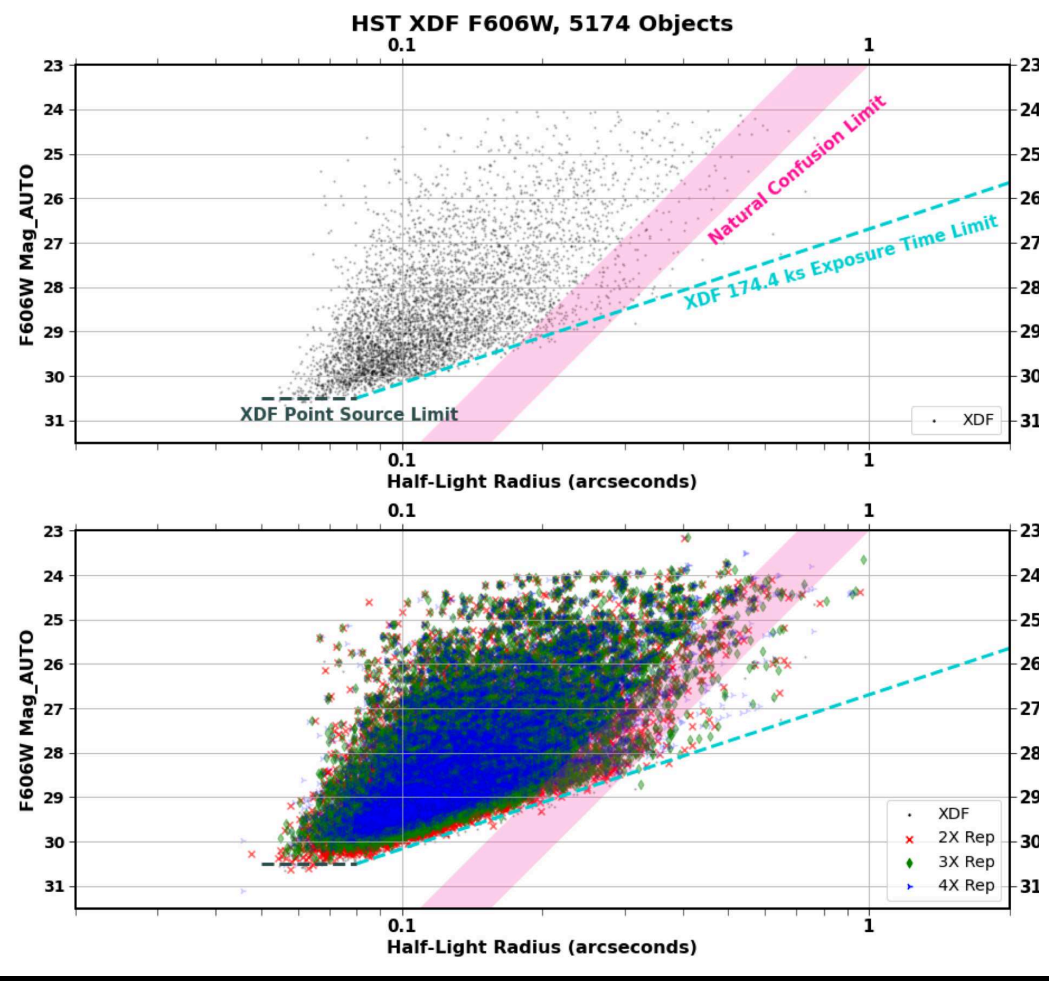

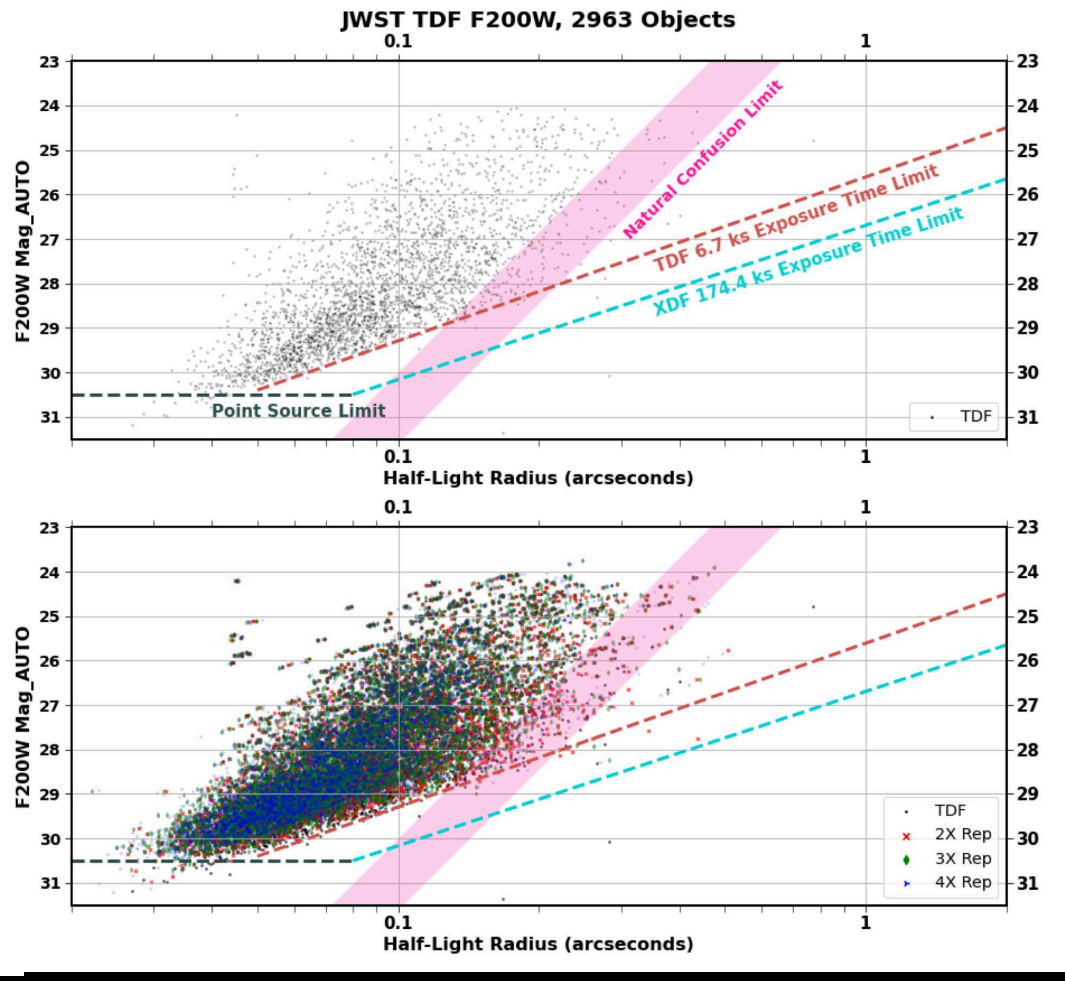

Top: AB-mag vs. r_e for 174 ksec HUDF (left) & 6.7 ksec TDF (right) galaxies.

Bottom: Same for HUDF & TDF rotated+replicated onto itself 2×, 3×, 4×.

- Flat spectrum point sources: 6.7 ksec JWST ∼as deep as 174 ksec HST!
- $\lesssim$35% of faintest galaxies lost due to object overlap (Kramer$^+$ 2022).
- Factor of ∼2–3 Diffuse Light not explained by missing faint galaxy pops.

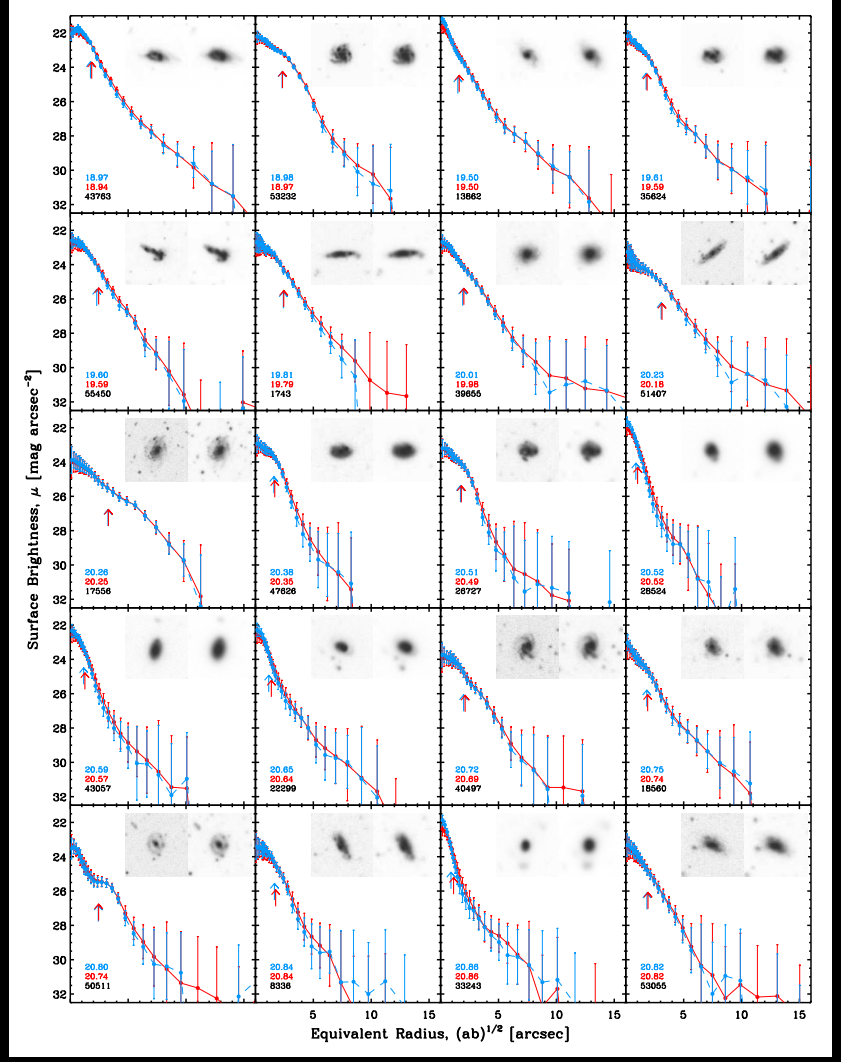

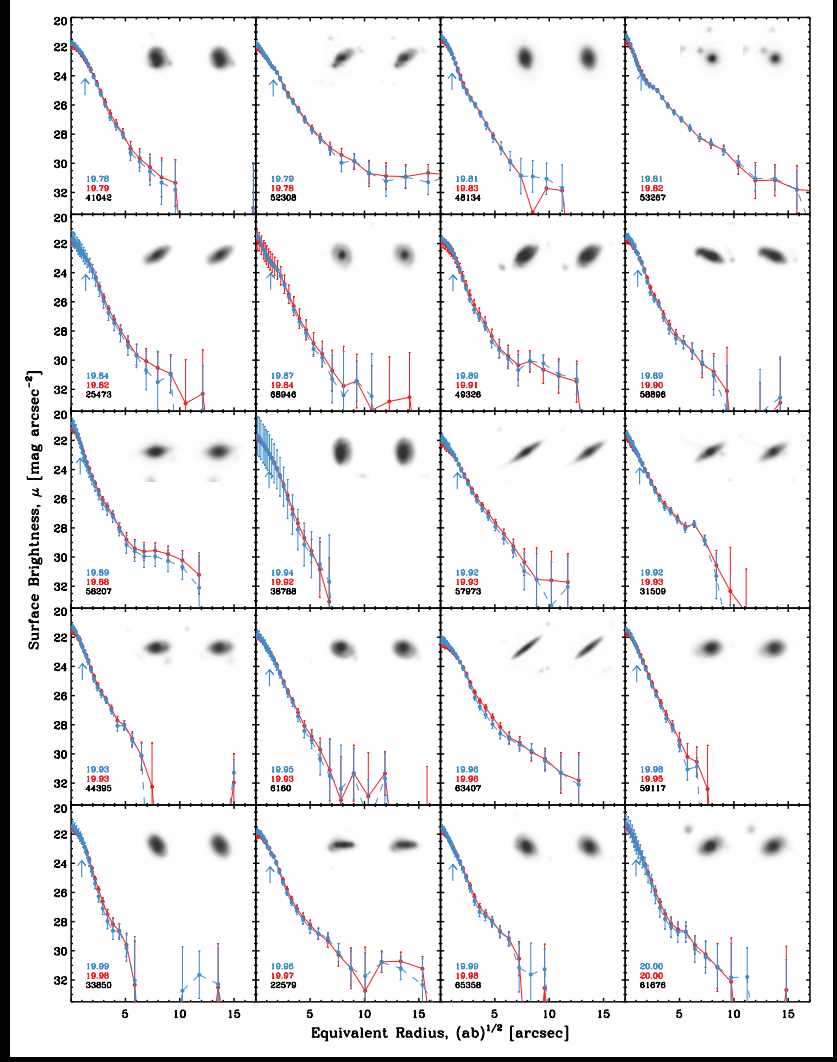

[Left]: LBT U-band, [Right] r-band: 20 of ∼300 galaxies with 17≲AB≲22 (*i.e.*, comprising *middle 50%* of EBL; Ashcraft^{+} 2018, 2022).

- 27-hr LBT stack to ≲32 mag/arcsec^2 shows on average ≲10-20% extra flux in galaxy outskirts compared to 6-hr best-seeing LBT stack.

$\Longrightarrow$ Factor of 2–3 diffuse light not likely hiding in dim galaxy outskirts!

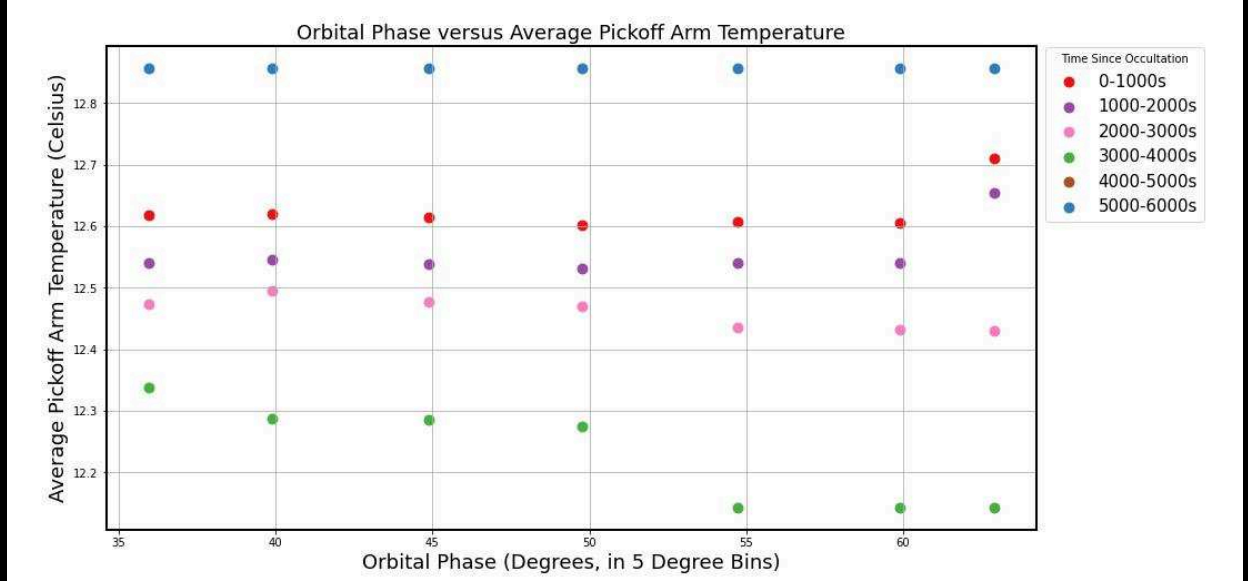

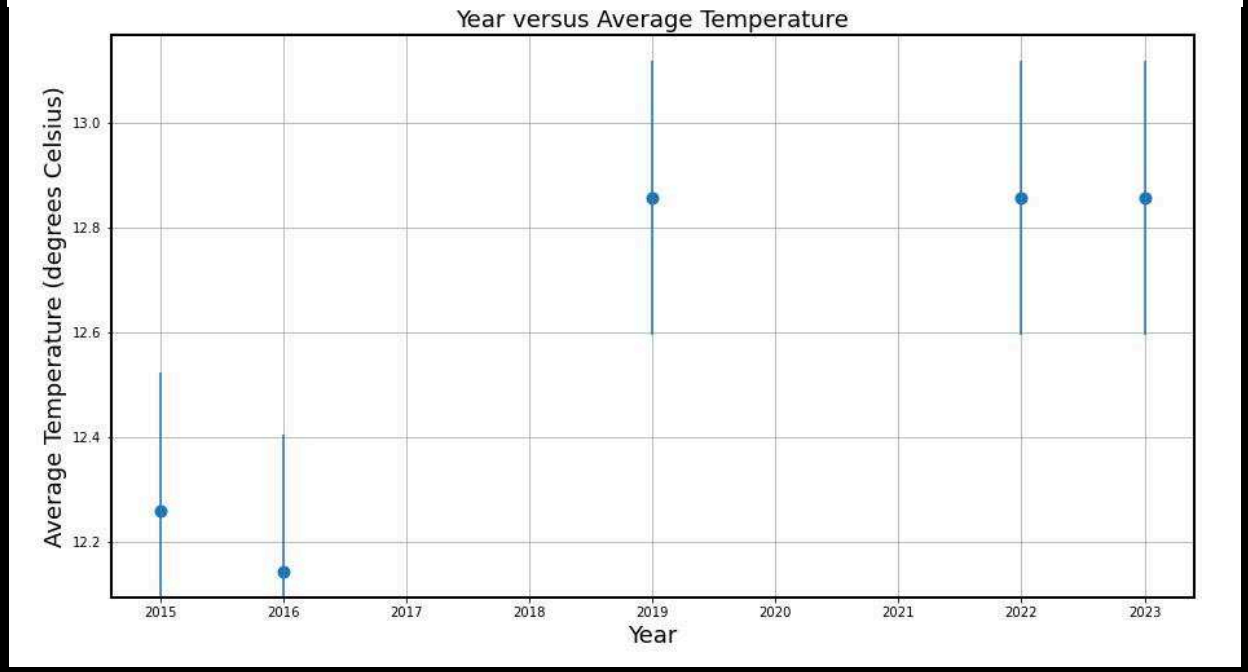

[Top] T(pickoff mirror) vs orbital phase & time since occultation: $\Delta T \lesssim 0.8$ C.

[Bottom] January T(pickoff mirror) vs. year: $\Delta T \simeq +0.6$ C — Solar Cycle?

- WFC3 Thermal Dark predictions accurate for $\Delta T \lesssim 1$ K (McIntyre, Carleton et al. 2023)

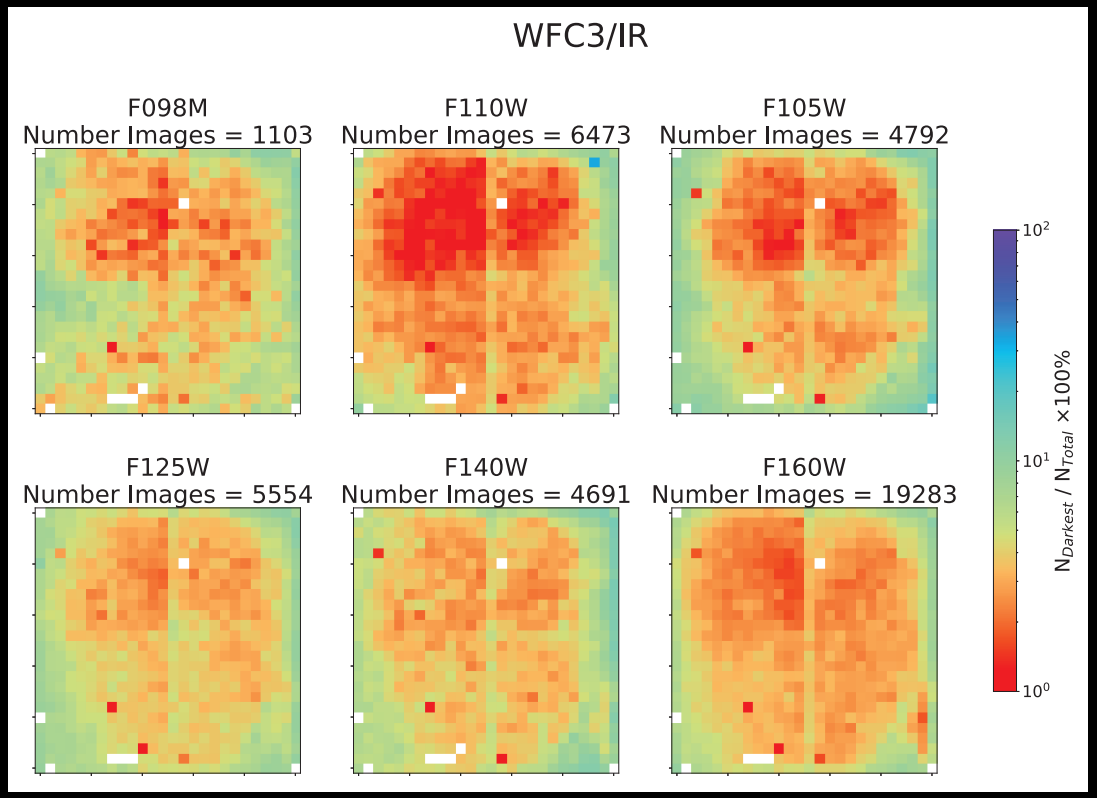

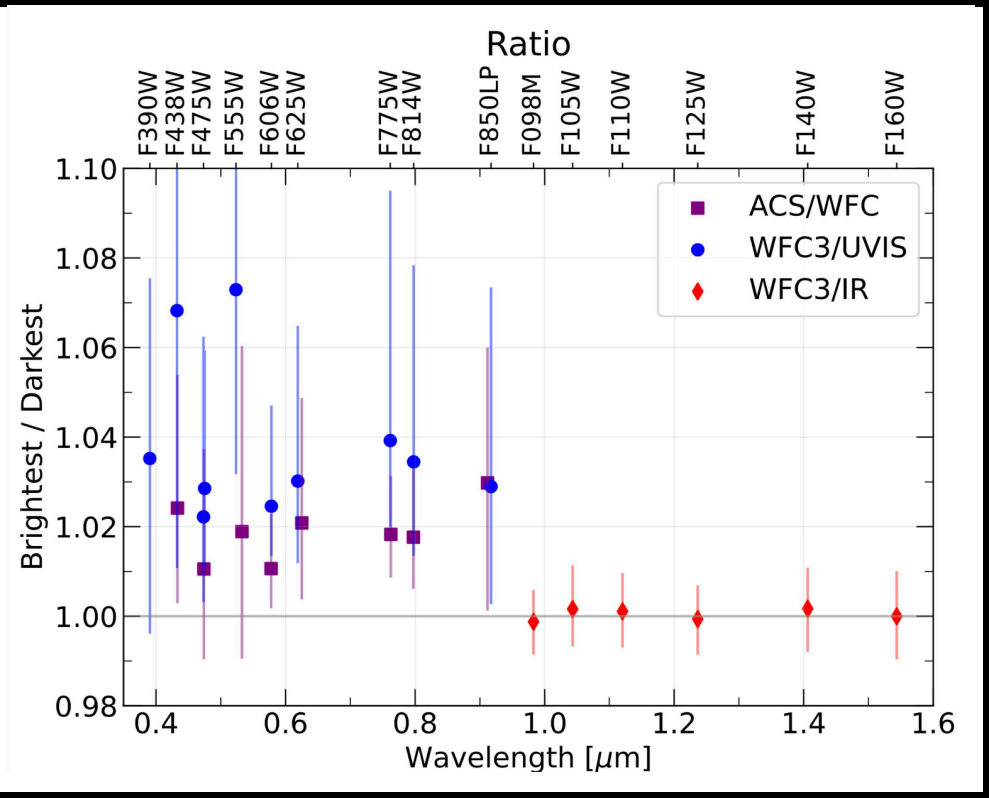

Left: Relative use of 676 WFC3/IR sky-SB boxes due to errors in delta-flats:

- Residual flat-field errors prefer some boxes over many thousands of fields.

Right: Residual FF errors: ACS: $\lesssim$2%; WFC3/UVIS: $\lesssim$4%; WFC3/IR: $\lesssim$1%

(O'Brien et al. 2023, AJ, in press; astro-ph/2210.08010)

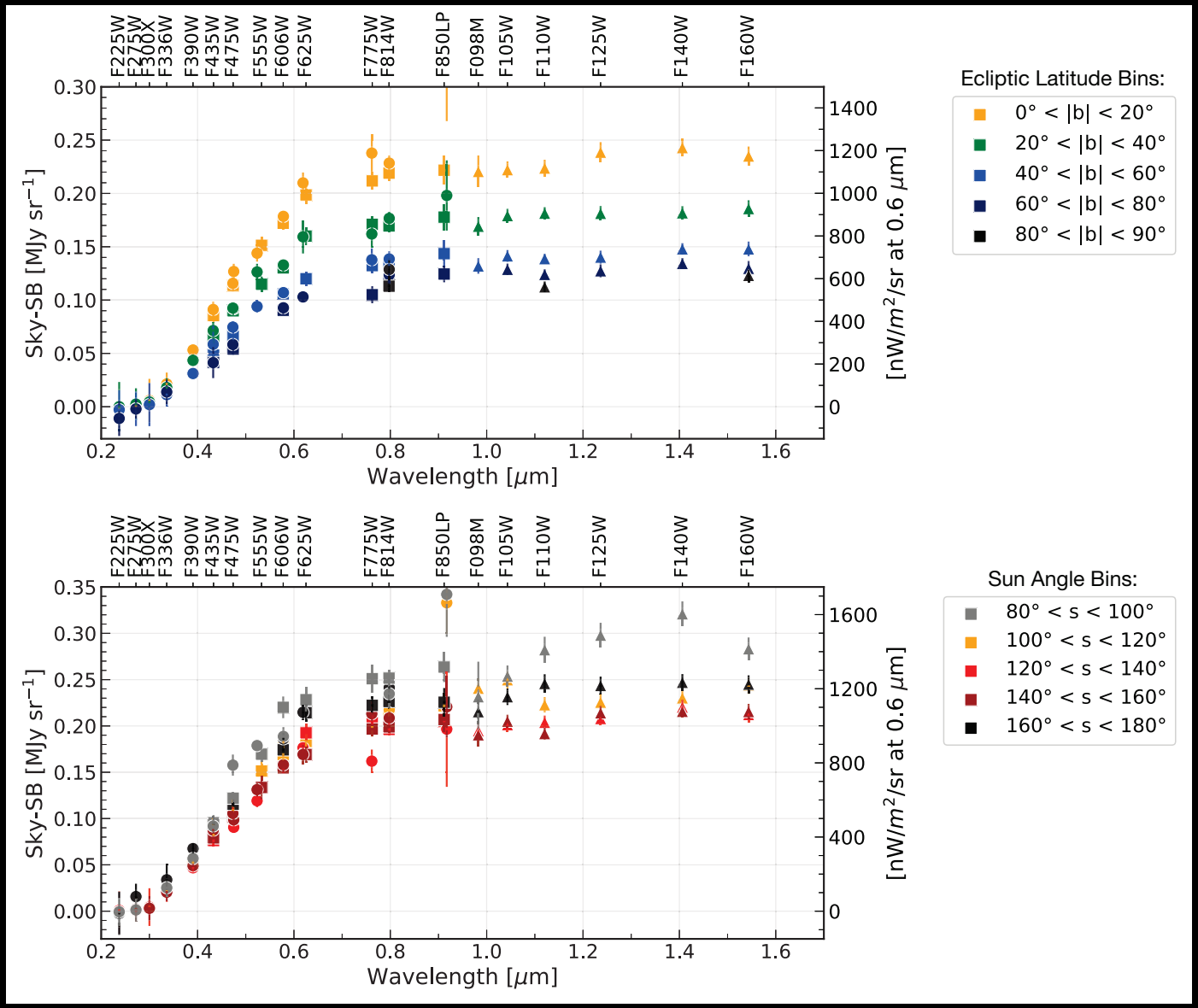

Top: Ecliptic Latitude dependence of panchromatic HST sky-SB.

Bottom: Sun Angle dependence of panchromatic HST sky-SB.

- Both show expected trends of higher sky-SB at lower $\boldsymbol{l}^{\mathbf{Ecl}}$/Sun-angles.

(O'Brien et al. 2023, AJ, in press; astro-ph/2210.08010)

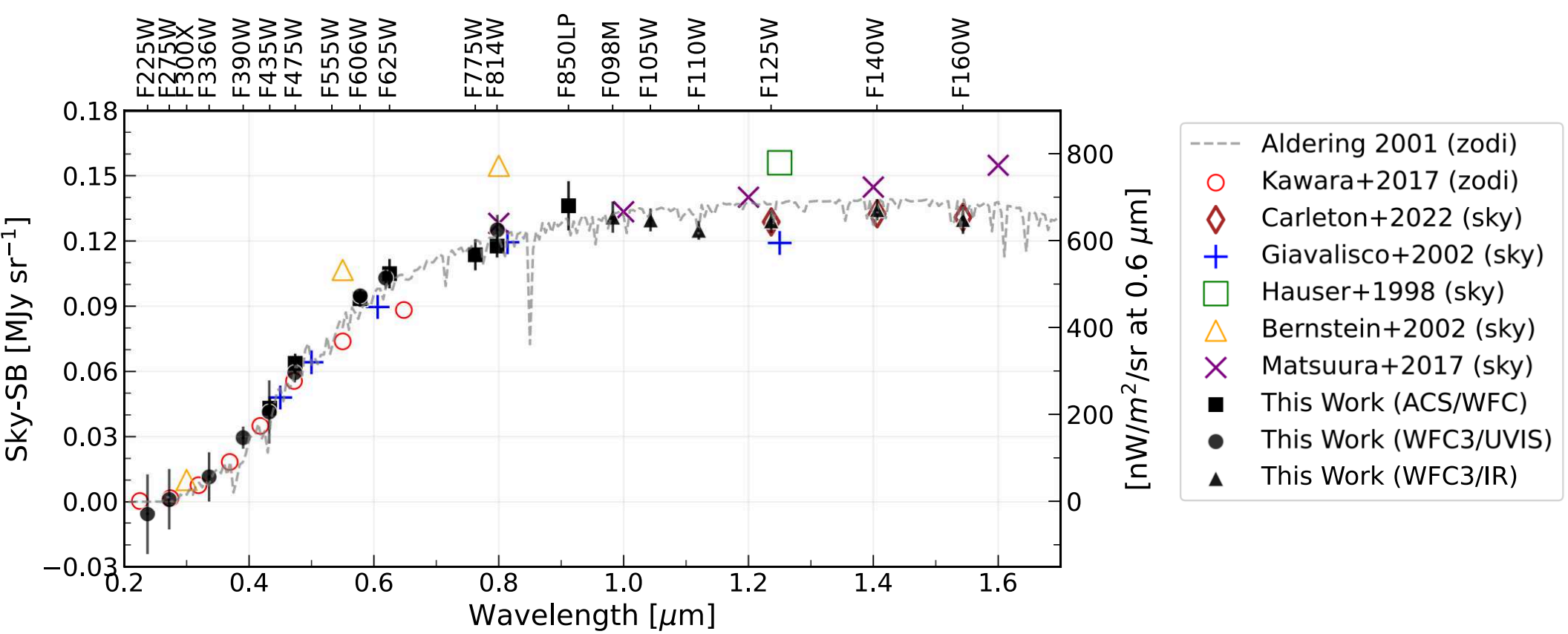

- We now have panchromatic HST Zodiacal sky-SB data at high-l^{Ecl}.
- Consistent with Aldering (2001), but HST a little bluer at 1.0–1.6 μm.
- Kelsall^{+} (1998) Zodiacal model needs update to include panchromatic HST+JWST 0.2–5 μm constraints.

(O'Brien et al. 2023, AJ, in press; astro-ph/2210.08010)

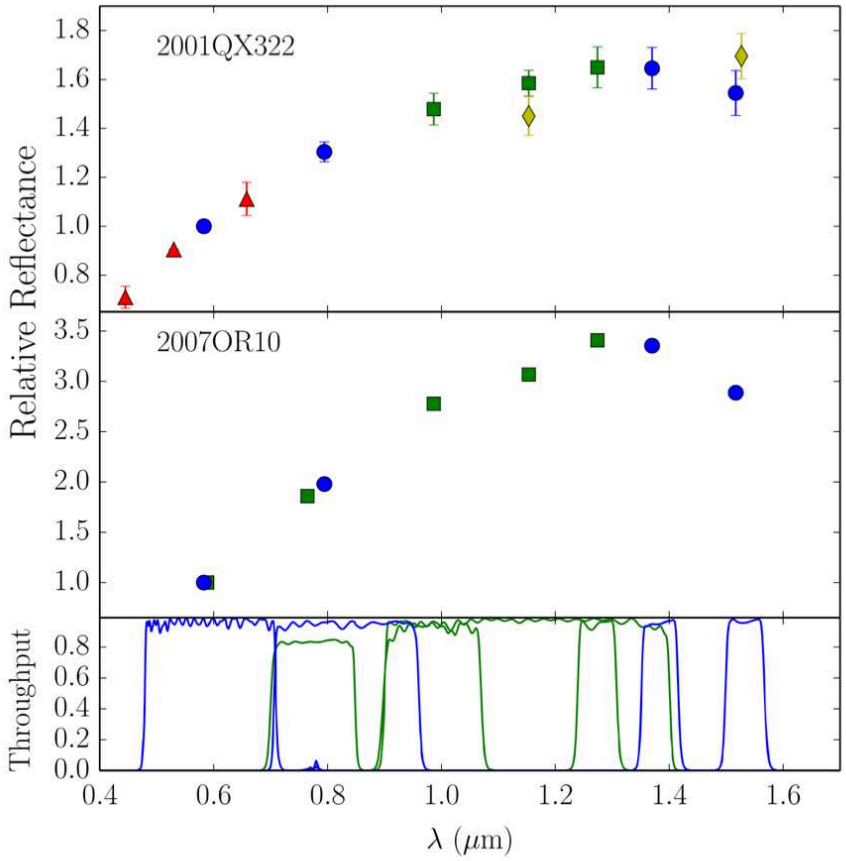

Figure 8. As in Figure 6. The yellow diamonds mark the spectra obtained for 2001 QX322 from the data presented by Benecchi et al. (2011). The F098m, F110w, and F127m photometry of 2001 QX322 have been vertically scaled for visible representation to match the F139m photometry and the photometry of Benecchi.

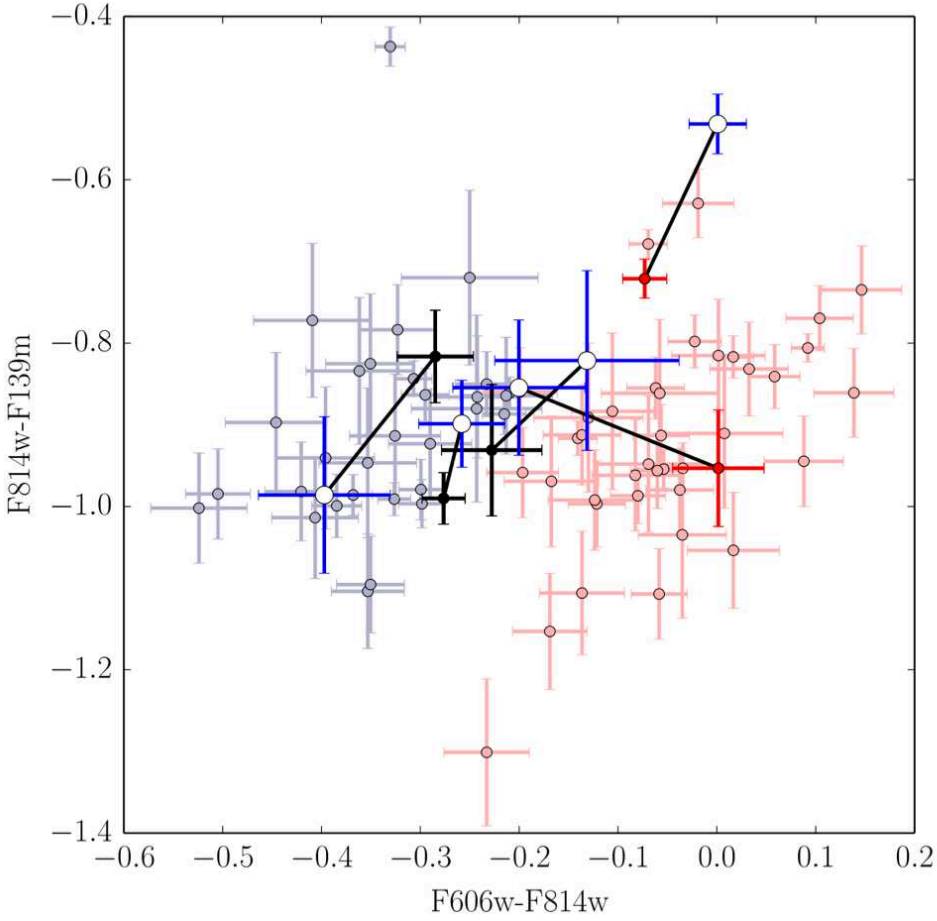

Figure 10. Observed and model optical and infrared colors of the five spectrally variable objects. The model cycle 18 colors are shown in blue points, while the observed cycle 17 colors are shown as solid red or black points according to their cycle 17 classification. Black lines connect the observed and model colors for each source. Gray and light red points show the full cycle 17 colors for comparison.

HST work on KBOs at 10–1000 AU show some remarkably blue IR colors.

Does OCC cometary dust in the inner solar system have similar albedos?

• References and other sources of material

Talk: http://www.asu.edu/clas/hst/www/jwst/skysurf_webbsurf_manchester23.pdf

Data: https://sites.google.com/view/jwstpearls and http://skysurf.asu.edu/

Carleton, T., Windhorst, R. A., O'Brien, R., et al. 2022, AJ, 164, 170 (astro-ph/2205.06347)

Cheng, C., Huang, J.-S., Smail, I., et al. 2023, ApJ, 942, L19 (astro-ph/2210.08163)

Diego, J. M., Meena, A. K., Adams, N. J., et al. A&A, 672, A3 (astro-ph/2210.06514)

Duncan, K. J., Windhorst, R. A., Koekemoer, A. M., et al. 2022, MNRAS, submitted (astro-ph/2212.09769)

Ferreira, L., Adams, N., Conselice, C. J., et al. 2022, ApJL, 938, L2 (astro-ph/2207.09428)

Jansen, R. A., et al. 2023, BAAS 241, 207.05 (iPoster at this mtg: HST+JWST NEP Time Domain Field)

Keel, W. C., Windhorst, R. A., Jansen, R. A., et al. 2022, AJ, 165, 166 (astro-ph/2208.14475)

Kramer, D. M., Carleton, T., Cohen, S. H., et al. 2022, ApJL, 940, L15 (astro-ph/2208.07218v2)

O'Brien, R., Carleton, T., Windhorst, R. et al. (2023, AJ, in press; astro-ph/2210.08010)

Windhorst, R., Cohen, S. H., Hathi, N. P., et al.2011, ApJS, 193, 27 (astro-ph/1005.2776)

Windhorst, R., Timmes, F. X., Wyithe, J. S. B., et al. 2018, ApJS, 234, 41 (astro-ph/1801.03584)

Windhorst, R. A., Carleton, T., O'Brien, R., et al. 2022, AJ, 164, 141 (astro-ph/2205.06214)

Windhorst, R. A., Cohen, S. H., Jansen, R. A., et al. 2023, AJ, 165, 13 (astro-ph/2209.04119)

Yan, H., Cohen, S. H., Windhorst, R. A., et al. 2023, ApJL, 942, L8 (astro-ph/2209.04092)

https://hubblesite.org/contents/news-releases/2022/news-2022-050

https://blogs.nasa.gov/webb/2022/10/05/webb-hubble-team-up-to-trace-interstellar-dust-within-a-galactic-pair/

https://blogs.nasa.gov/webb/2022/12/14/webb-glimpses-field-of-extragalactic-pearls-studded-with-galactic-diamonds/

https://esawebb.org/images/pearls1/zoomable/